Precise Measurement of the Neutron Magnetic Form Factor

G.P.Gilfoyle, J.D.Lachniet, W.K.Brooks, M.F.Vineyard, B.Quinn (the E5 group),*

and the CLAS Collaboration

Outline:

1. Motivation.
2. Necessary Background.
3. Previous Measurements.
4. Measuring G_M^n.
5. Results.
6. Current Status and the Future.
7. Conclusions.

* Thesis project.

Scientific Motivation

- The neutron magnetic form factor $G_M^n(Q^2)$ is a fundamental observable related to the spatial distribution of the charge and magnetization in the neutron.

Scientific Motivation

- The neutron magnetic form factor $G_M^n(Q^2)$ is a fundamental observable related to the spatial distribution of the charge and magnetization in the neutron.
- Part of a broad effort to answer the question 'What is the internal landscape of the nucleons?'.*

* 'The Frontiers of Nuclear Science: A Long-Range Plan', NSF/DOE Nuclear Science Advisory Committee, December, 2007.

Scientific Motivation

- The neutron magnetic form factor $G_M^n(Q^2)$ is a fundamental observable related to the spatial distribution of the charge and magnetization in the neutron.
- Part of a broad effort to answer the question 'What is the internal landscape of the nucleons?'.*
- The elastic electromagnetic form factors (EEFFs) G_M^n, G_E^n, G_M^p, and G_E^p constrain the generalized parton distributions (GPDs) which promise to give us a three-dimensional picture of hadrons.

$*$ 'The Frontiers of Nuclear Science: A Long-Range Plan', NSF/DOE Nuclear Science Advisory Committee, December, 2007.

Scientific Motivation

- The neutron magnetic form factor $G_M^n(Q^2)$ is a fundamental observable related to the spatial distribution of the charge and magnetization in the neutron.
- Part of a broad effort to answer the question ‘What is the internal landscape of the nucleons?’.*
- The elastic electromagnetic form factors (EEFFs) G_M^n, G_E^n, G_M^p, and G_E^p constrain the generalized parton distributions (GPDs) which promise to give us a three-dimensional picture of hadrons.
- EEFFs are a fundamental and early challenge for lattice QCD.

* ‘The Frontiers of Nuclear Science: A Long-Range Plan’, NSF/DOE Nuclear Science Advisory Committee, December, 2007.

Scientific Motivation

- The neutron magnetic form factor $G_M^n(Q^2)$ is a fundamental observable related to the spatial distribution of the charge and magnetization in the neutron.
- Part of a broad effort to answer the question 'What is the internal landscape of the nucleons?'.*
- The elastic electromagnetic form factors (EEFFs) G_M^n, G_E^n, G_M^p, and G_E^p constrain the generalized parton distributions (GPDs) which promise to give us a three-dimensional picture of hadrons.
- EEFFs are a fundamental and early challenge for lattice QCD.

We present new data with precision and coverage that eclipse the world's data in this Q^2 range.

* 'The Frontiers of Nuclear Science: A Long-Range Plan', NSF/DOE Nuclear Science Advisory Committee, December, 2007.

Some Necessary Background

- Use the Dirac (F_1) and Pauli (F_2) form factors for the cross section.

$$\frac{d\sigma}{d\Omega} = \sigma_{Mott}\left[\left(F_1^2 + \kappa^2 \tau F_2^2\right) + 2\tau\left(F_1 + \kappa F_2\right)^2 \tan^2\left(\frac{\theta}{2}\right)\right]$$

where κ is the anomalous magnetic moment, E (E') is the incoming (outgoing) electron energy, θ is the scattered electron angle, and

$$\tau = \frac{Q^2}{4M^2} \qquad \sigma_{Mott} = \frac{\alpha^2 E' \cos^2(\frac{\theta}{2})}{4E^3 \sin^4(\frac{\theta}{2})} \quad .$$

- For convenience use the Sachs form factors.

$$\frac{d\sigma}{d\Omega} = \sigma_{Mott}\left(\frac{(G_E^n)^2 + \tau(G_M^n)^2}{1+\tau} + 2\tau \tan^2\frac{\theta}{2}(G_M^n)^2\right)$$

$$G_E = F_1 - \tau F_2 \qquad G_M = F_1 + F_2$$

More Background - Interpreting the EEFFs

- At low momentum transfer ($Q^2 \ll M_N^2$) G_E and G_M are the Fourier transforms of the densities of charge and magnetization.

$$G_E(Q^2) = \int \rho(r) e^{-i\vec{q}\cdot\vec{r}} d^3 r$$

where $\vec{q}$ is the 3-momentum transferred by the electron.

- At high Q^2 relativistic effects make the interpretation more interesting!

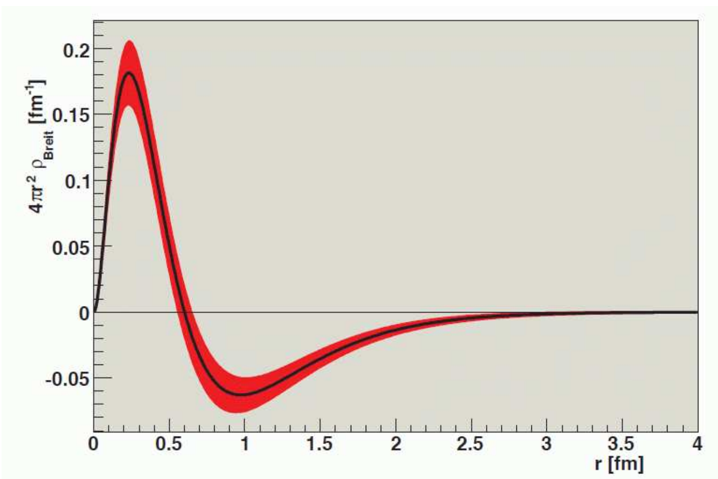

NSAC Long Range Plan

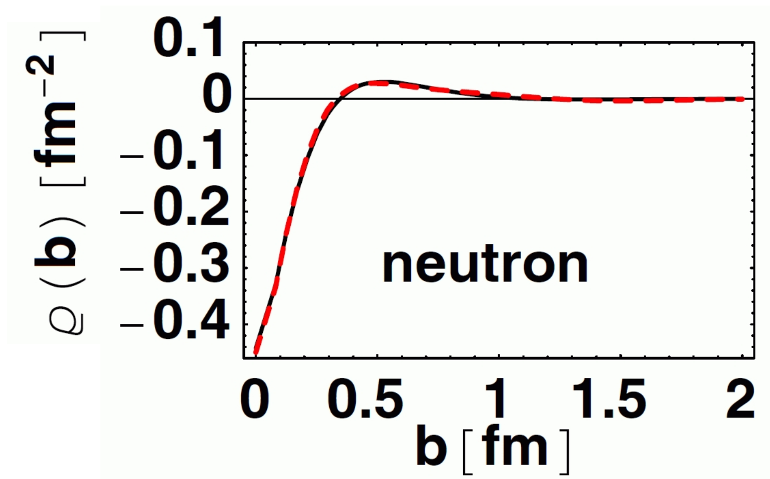

G.A.Miller, Phys.Rev.Lett.99:112001,2007

Early Measurements of EEFFs

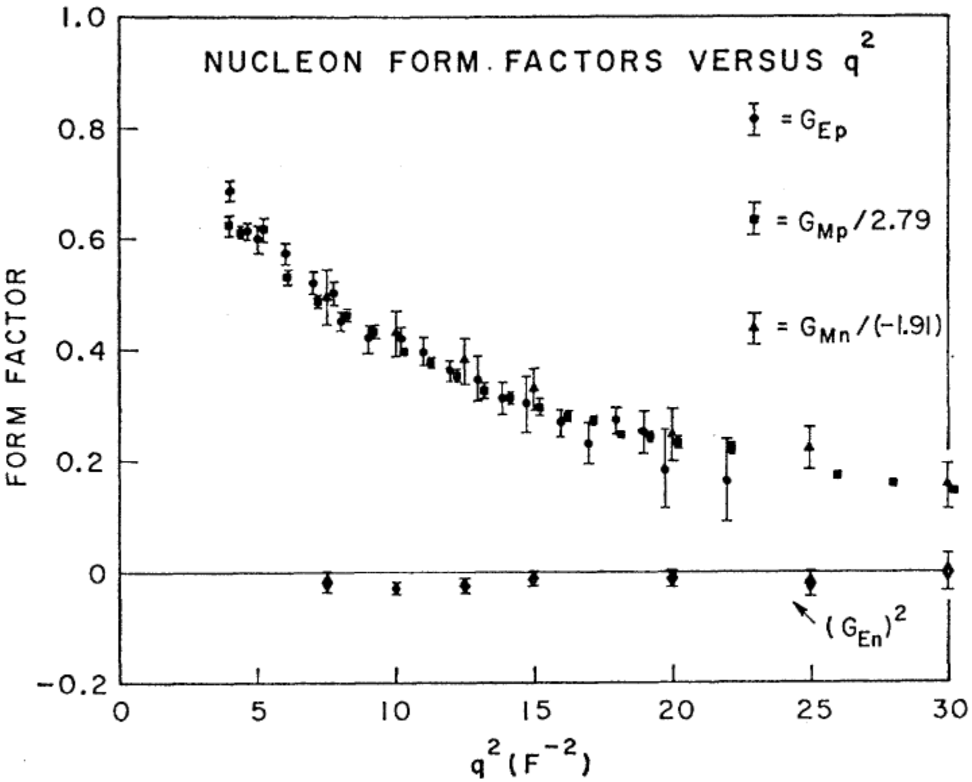

Phys. Rev. 139, B458, 1965.

$$G_E^p \approx G_M^p/\mu_p \approx G_M^n/\mu_n \approx G_D \quad G_E^n \approx 0 \quad G_D = \frac{1}{\left(1 + \frac{Q^2}{\Lambda}\right)^2} \quad \Lambda = 0.71\,\mathrm{GeV}^2$$

The dipole form factor G_D corresponds to an exponential drop with r in the charge and magnetization densities.

Current World Data on EEFFs

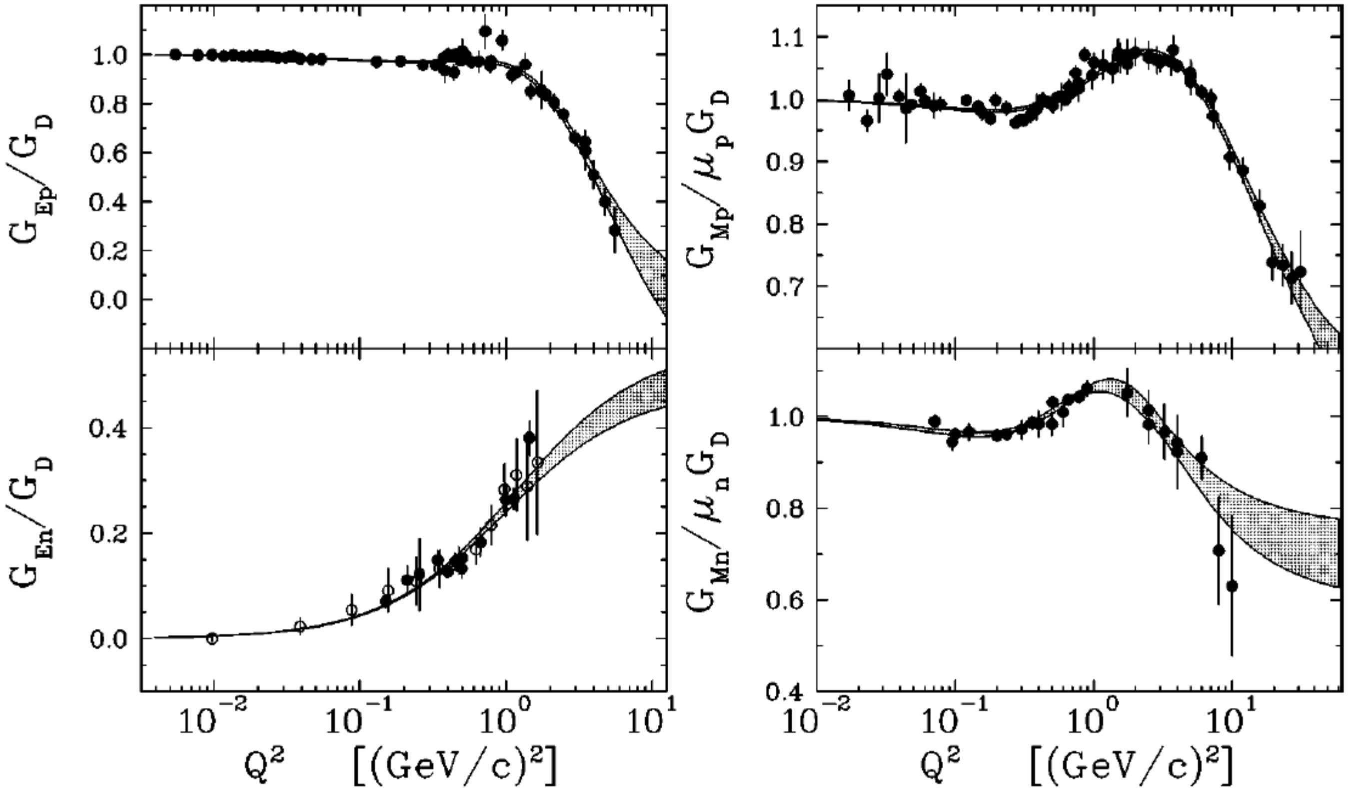

J.J.Kelly, Phys. Rev.C, 068202, 2004.

- Proton form factors have small uncertainties and reach higher Q^2.
- Neutron form factors are sparse and have large uncertainties.
- Significant deviations from the dipole form factor.

Measuring G_M^n

- Early methods:
  - Neutrons on atomic electrons (V.E. Krohn and G.R. Ringo, Phys. Rev. 148 (1966) 1303).
  - Quasielastic $D(e,e')D$ and $D(e,e'n)p$: Use models to extract G_M^n; uncertainties $\approx 5\% - 20\%$.
- Modern methods:
  - Ratio of $e-n/e-p$ scattering from deuterium; more below.
  - Quasielastic $^3\vec{\mathrm{He}}(\vec{e},e')^3\mathrm{He}$: Constrain calculations of nuclear effects with other measurements ($A_{T'}$) for $Q^2 < 1\ \mathrm{GeV}^2$.

M. Jones, 2005 Hall C Workshop.

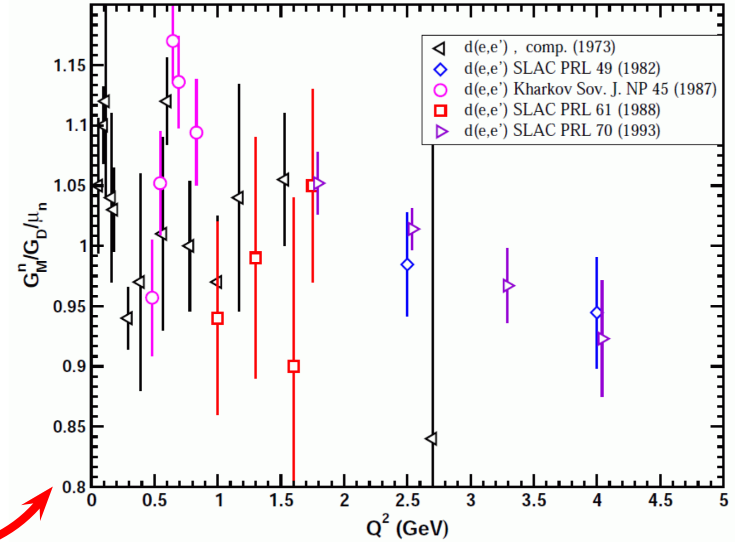

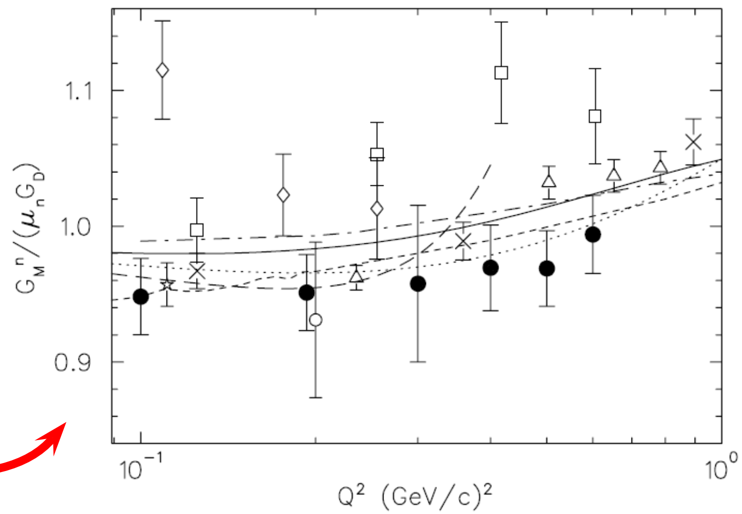

Anderson et al., PRC, 75, 034003, 2007.

Measuring G_M^n - The Ratio Method

- Without a free neutron target we use deuterium and measure R

$$R = \frac{\frac{d\sigma}{d\Omega}[^2\mathrm{H}(e,e'n)_{QE}]}{\frac{d\sigma}{d\Omega}[^2\mathrm{H}(e,e'p)_{QE}]}$$

$$= a(E,Q^2,\theta_{pq}^{max},W_{max}^2) \times \frac{\sigma_{Mott}\left(\frac{(G_E^n)^2+\tau(G_M^n)^2}{1+\tau} + 2\tau\tan^2\frac{\theta}{2}(G_M^n)^2\right)}{\frac{d\sigma}{d\Omega}[^1\mathrm{H}(e,e')p]}$$

where $a(E,Q^2,\theta_{pq}^{max},W_{max}^2)$ corrects for nuclear effects, θ_{pq}^{max} and W_{max}^2 are kinematic cuts, and the numerator is the precisely-known proton cross section.

- Less vulnerable to nuclear structure (*e.g.*, deuteron model, *etc.*) and experimental effects (*e.g.*, electron acceptance, *etc.*).
- Must accurately measure the nucleon detection efficiencies and match the geometric solid angles.

The Experiment- Jefferson Lab

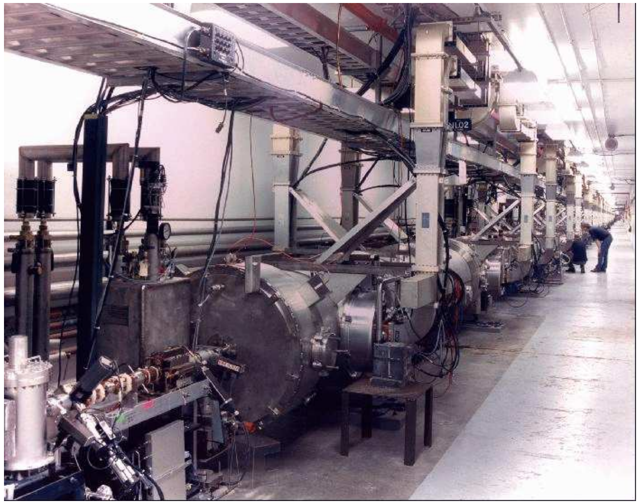

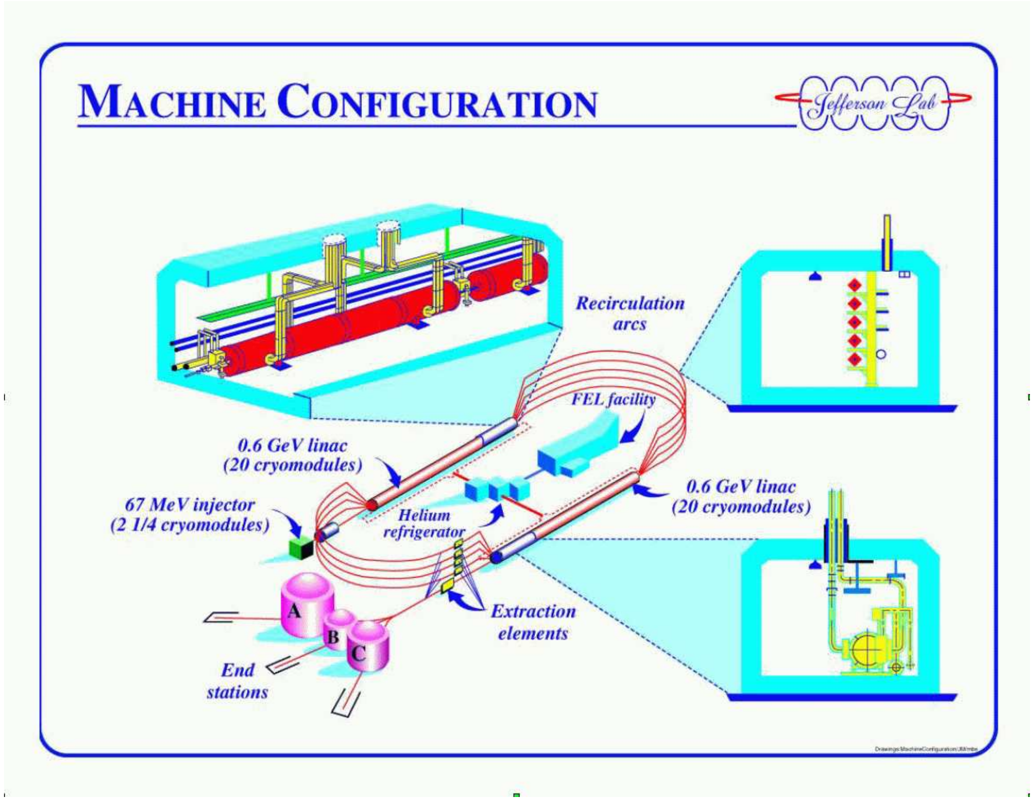

Continuous Electron Beam Accelerator Facility (CEBAF)

- Superconducting Electron Accelerator (338 cavities), 100% duty cycle.
- $E_{max} = 6$ GeV, $\Delta E/E = 10^{-4}$, $I_{max} = 200\ \mu A$, $P_e \geq 80\%$.

The Experiment - JLab End Stations

Hall A - Two identical, high-resolution spectrometers ($\Delta p/p < 2 \times 10^{-4}$); luminosity $\approx 10^{38}\ cm^{-2} s^{-1}$.

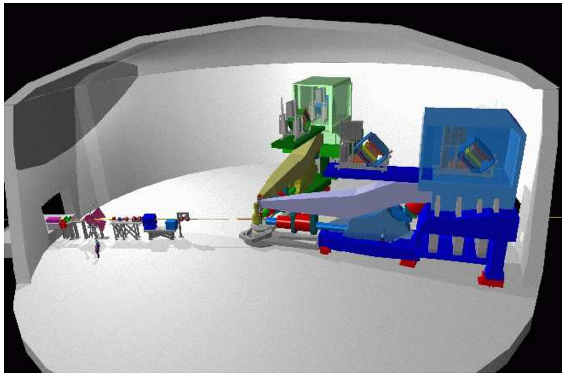

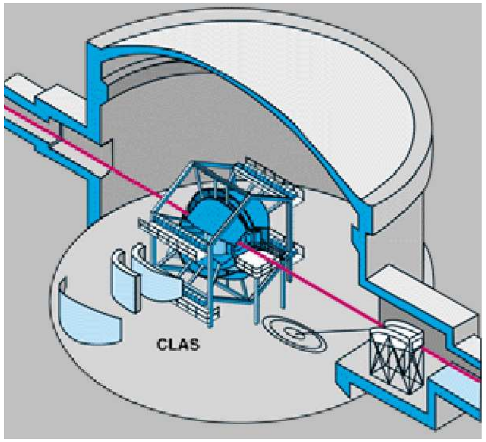

Hall B - The CLAS, nearly 4π-acceptance spectrometer based on a toroidal magnet ($\Delta p/p = 0.5\%$); luminosity $\approx 10^{34}\ cm^{-2} s^{-1}$.

Hall C - Moderate-resolution (10^{-3}), 7-GeV/c High-Momentum Spectrometer (HMS) and the large-acceptance Short-Orbit Spectrometer (SOS) and additional detectors.

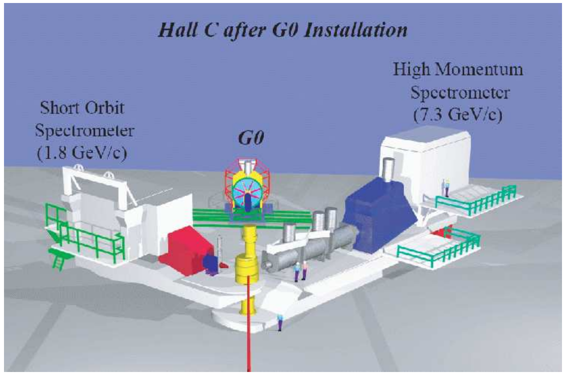

The Experiment - CLAS

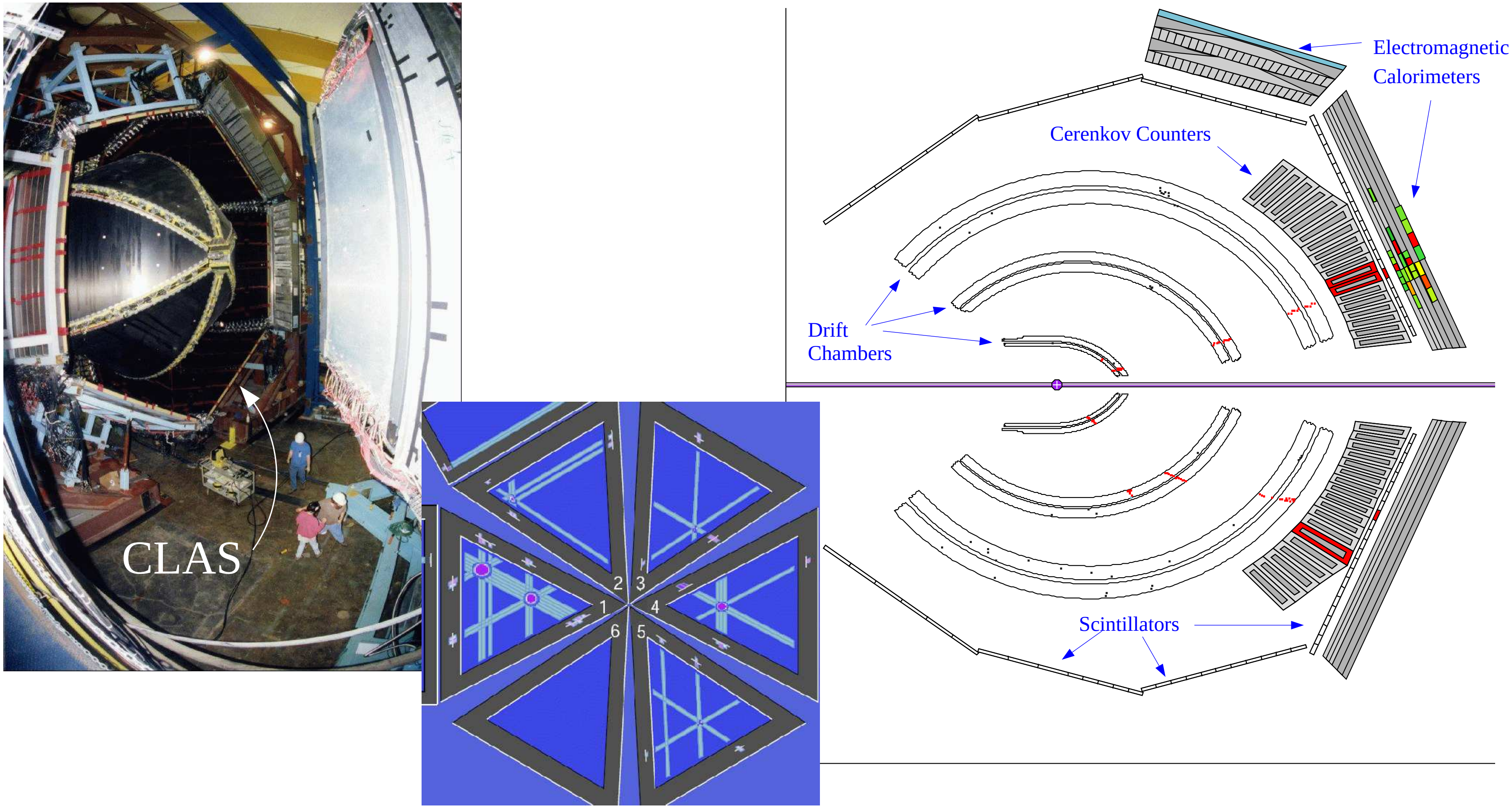

Six identical mass spectrometers.

Charged particle angles: $8^\circ - 144^\circ$.

Momentum resolution: $\approx 0.5\%$ (charged).

Particle ID: p, π^+/π^-, K^+/K^-, e^+/e^-.

Neutral particle angles: $8^\circ - 70^\circ$.

Angular resolution: $\approx 0.5\ mr$ (charged).

Experimental Details - E5 Data Set

- Data Set:
  - 2.3 billion triggers.
  - $\mathrm{E} = 4.2\ \mathrm{GeV}$ and $2.6\ \mathrm{GeV}$ with positive torus polarity (electrons inbending).
  - $\mathrm{E} = 2.6\ \mathrm{GeV}$ with negative torus polarity (electrons outbending).
- Dual target cell with liquid hydrogen and deuterium separated by 4.7-cm. Perform *in situ* calibrations during data collection.
- Targets are well separated.

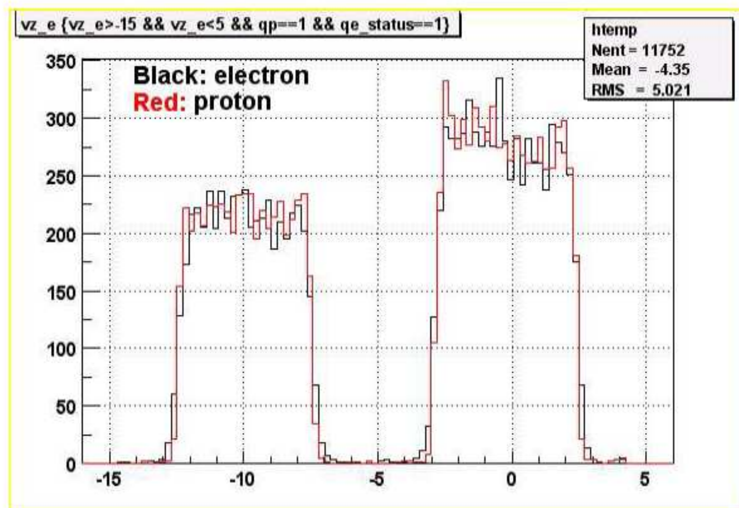

The Ratio Method - Selecting Quasielastic Events

- Kinematic definitions.

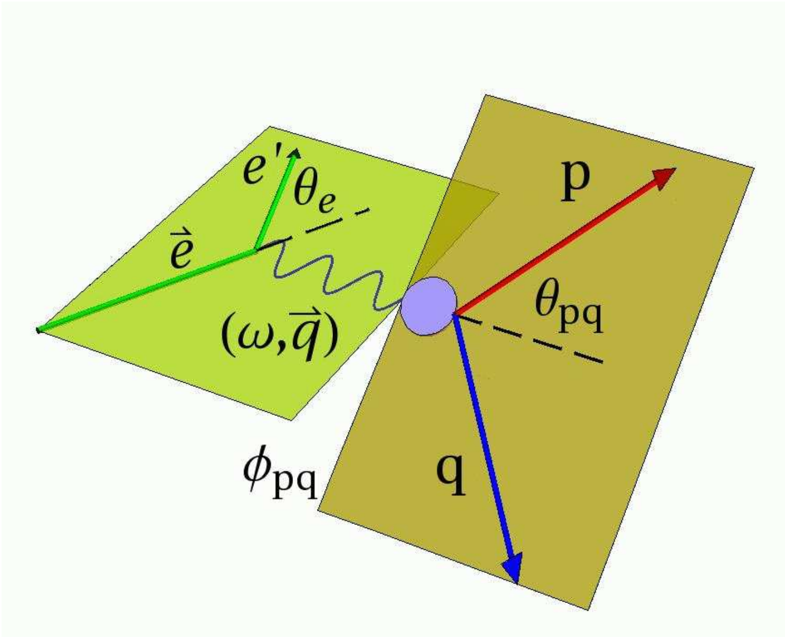

- Quasielastic (QE) events cluster in a cone around $\theta_{pq} \approx 0^\circ$. Simulation shows effect of requiring $\theta_{pq}^{max} = 3^\circ$. See L. Durand, Phys. Rev. 115, 1020 (1959).

- Use the same QE cut for protons and neutrons.

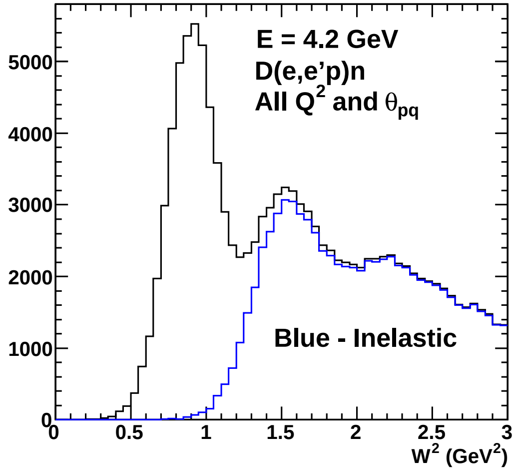

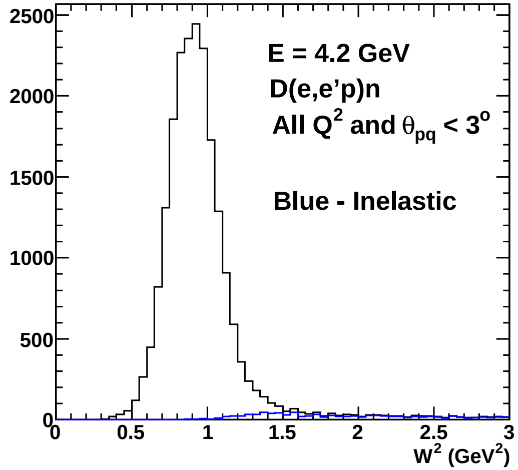

Analysis - Event Selection

- Use $e-n/e-p$ ratio to reduce systematic uncertainties.
- $e-p$ selection: 'standard' CLAS analysis for electrons and protons .
- $e-n$ selection: same criteria for electrons; TOF and calorimeter (EC) are TWO, INDEPENDENT neutron measurements.
- Quasi-elastic event selection: Apply a maximum θ_{pq} cut to eliminate inelastic events plus a cut on W^2.
- Acceptance matching: Use the quasi-elastic electron kinematics to predict if the nucleon (proton or neutron) lies in CLAS acceptance. Require both hypotheses to be satisfied.

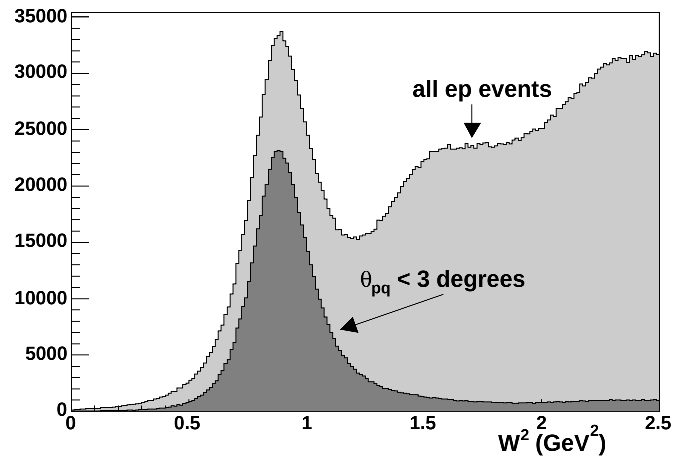

- Neutrons and protons treated exactly the same whenever possible.

Neutron Detection Efficiency (NDE): EC

Neutron detection efficiency (NDE):

1. Use the $ep \to e'\pi^+ n$ reaction from the hydrogen target for tagged neutrons in the TOF and EC; standard CLAS cuts for electrons.
2. For π^+, use positive tracks, cut on the difference between β measured from tracking and from time-of-flight.
3. For neutrons, $ep \to e'\pi^+ X$ for $0.9 < m_X < 0.95\,\mathrm{GeV/c^2}$.
4. In the calorimeter use the neutron momentum $\vec{p}_n$ to determine the location of a hit in the fiducial region (reconstructed event) and search for that neutron (a found event if it's there).

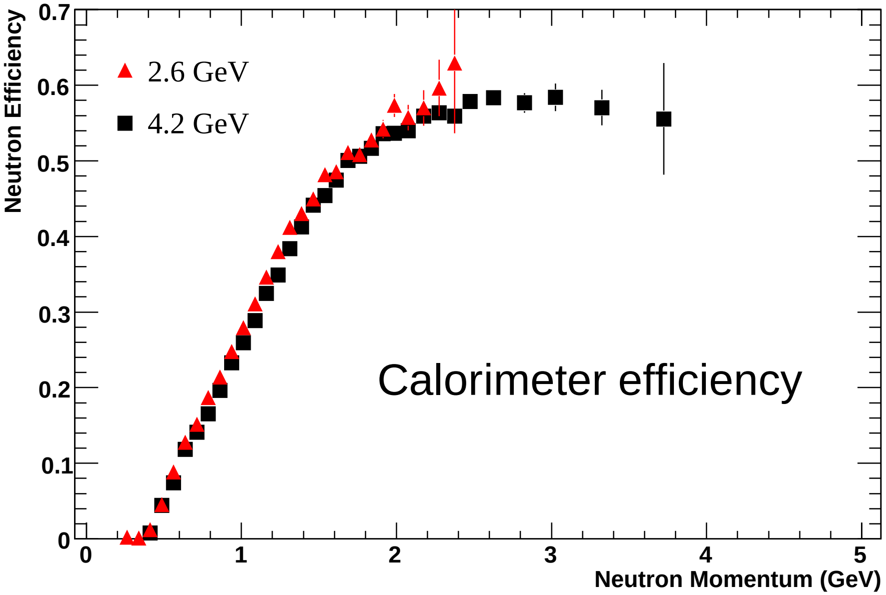

Neutron Detection Efficiency (NDE): TOF

1. Use the same $ep \to e'\pi^+ n$ reaction from hydrogen for tagged neutrons.
2. In the TOF use the neutron momentum $\vec{p}_n$ to predict which TOF paddle is hit (reconstructed event) and then search (a found event if it's there).

We have two measurements of the NDE (EC and TOF) for each set of running conditions.

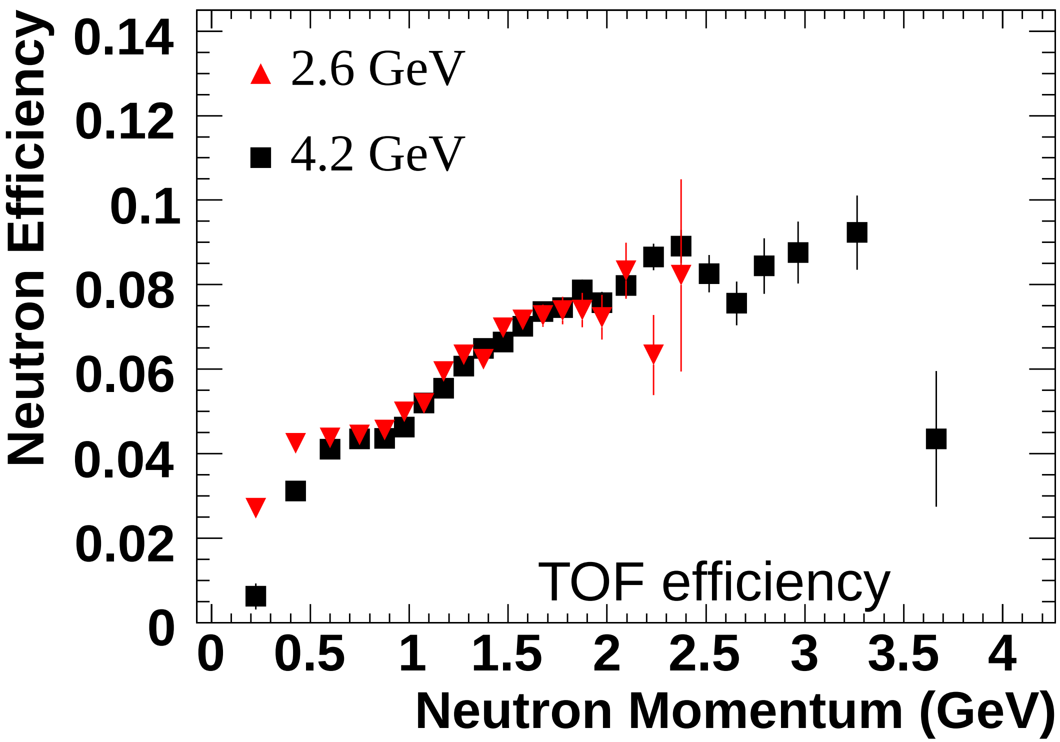

Proton detection efficiency

1. Use $ep \rightarrow e'p$ elastic scattering from hydrogen for tagged protons.
2. Standard CLAS cuts for electrons; W^2 cut to select ep elastics.
3. Protons identified as positive tracks with a coplanarity cut.
4. In the TOF use the missing momentum from $ep \rightarrow e'X$ to predict the TOF paddle that will be struck by the proton (a reconstructed event). Search that paddle or an adjacent one for a positively-charged particle (a found event if it's there). Results below are for sector 1.

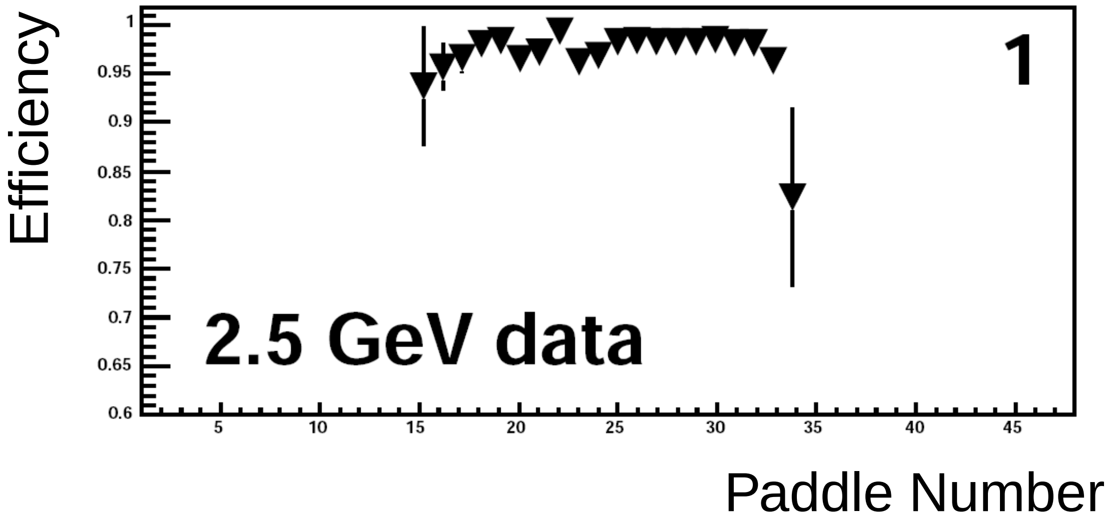

Additional Corrections

- Nuclear effects: The $e - n/e - p$ ratio for free nucleons differs from the one for bound nucleons. Recall the factor $a(E, Q^2, \theta_{pq}^{max}, W_{max}^2)$ in R. Calculations by Jeschonnek and Arenhövel were close to unity.
- Radiative corrections: Calculated for exclusive $D(e, e'p)n$ with the code EXCLURAD (CLAS-Note 2005-022 and PRD, 66, 074004, 2002). Ratio close to unity.
- Fermi motion in the target: Causes nucleons to migrate out of the CLAS acceptance. Effect was simulated to determine correction.
- Momentum corrections.
- Effect of θ_{pq}^{max}.

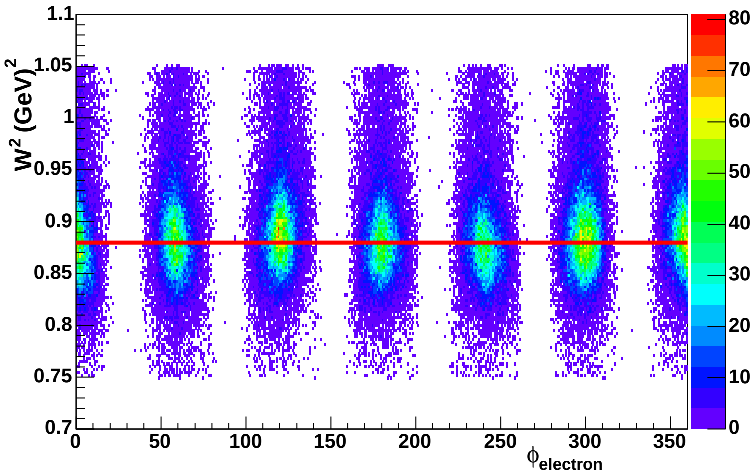

Systematic Uncertainties

Quantity	2.6 GeV (%)	4.2 GeV (%)	Quantity	2.6 GeV (%)	4.2 GeV (%)
Calorimeter neutron efficiency parameter-ization	< 1.5	< 1.0	TOF neutron effi-ciency parameter-ization	< 2.0	< 3.2
proton σ	< 1.0	< 1.5	G_E^n	< 0.5	< 0.7
Fermi loss correction	< 0.8	< 0.9	θ_{pq} cut	< 0.4	< 1.0
neutron accidentals	< 0.07	< 0.3	neutron MM cut	< 0.5	< 0.07
neutron proximity cut	< 0.22	< 0.15	proton efficiency	< 0.3	< 0.35
Nuclear Corrections	< 0.17	< 0.2	Radiative correc-tions	< 0.05	< 0.06

Upper limits on percent estimated systematic uncertainty for different contributions.

Goal: Systematic uncertainty less than 3% on G_M^n.

Systematic Uncertainties - NDE

- Calorimeter neutron detection efficiency (NDE) parameterization:
  1. NDE fitted with a third order polynomial plus a flat region at higher momentum.
  2. Highest order term was dropped and the ratio R regenerated.
  3. The upper limit on the range of values of R extracted from the different NDE fits was assigned as the systematic uncertainty.
- TOF NDE parameterization: Similar to calorimeter extraction except the second and third order terms in the polynomial were dropped.
- These are the largest contributions from this measurement.

Detector	2.6 GeV	4.2 GeV
Calorimeter	<1.5	<1.0
TOF	<2.0	<3.2

Percentage systematic uncertainties in neutron detection efficiency parameterization.

Systematic Uncertainties - Proton Cross Section

- Calculate $\delta\sigma_p$, the uncertainty on the proton cross section σ_p, as the difference between the Arrington (Phys. Rev. C 68, 034325, 2003) and Bosted (Phys. Rev. C, 51:409-411, 1995) parameterizations.
- The left-hand panel shows $\delta\sigma_p$. The parameterizations cross at $Q^2 \approx 1.1\ \mathrm{GeV}^2$ so a value of $\delta\sigma_9$ was assigned based on the behavior of $\delta\sigma_p$ at higher Q^2.

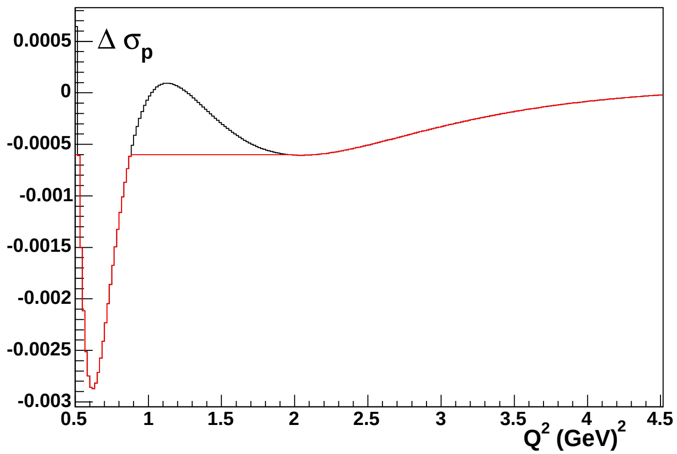

Red curve - Assigned value of $\delta\sigma_p$.

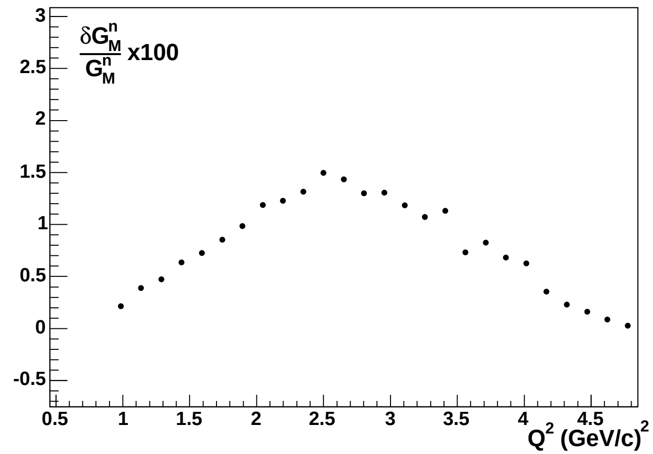

Fractional uncertainty due to $\delta\sigma_p$ at 4.2 GeV.

Systematic Uncertainties - Fermi Motion

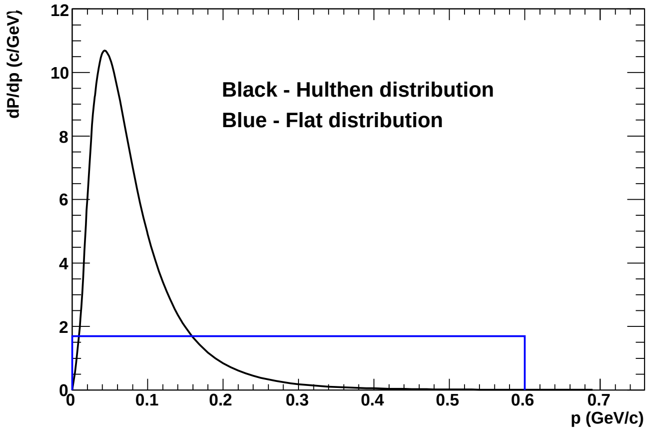

Nucleon momentum distributions.

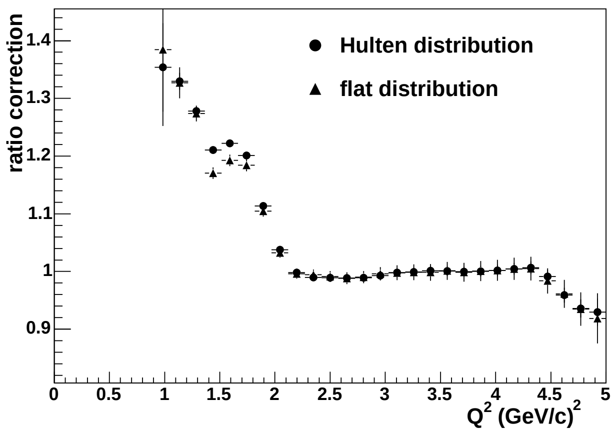

Correction factors for R at 4.2 GeV.

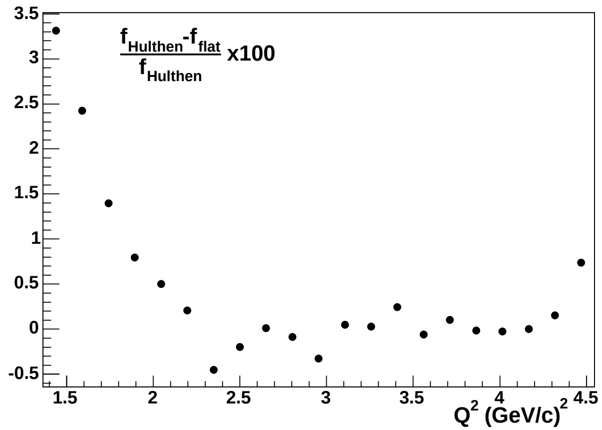

Fractional difference in the ratio correction factor obtained from the Hulthen and flat nucleon momentum distributions.

Results - Overlaps and Final Averages

- The ratio R for each beam energy is the weighted average of the EC and TOF measurements.
- Overlapping measurements of reduced G_M^n are consistent.
- Systematic uncertainty $\frac{\delta G_M^n}{G_M^n} \times 100 < 2.5\%$.

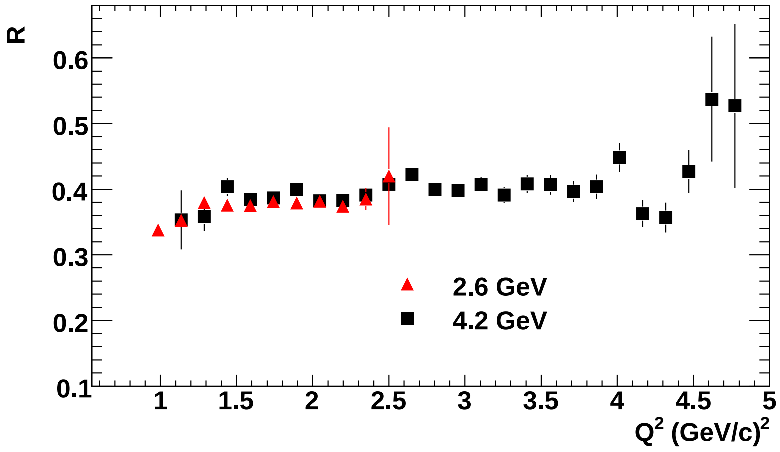

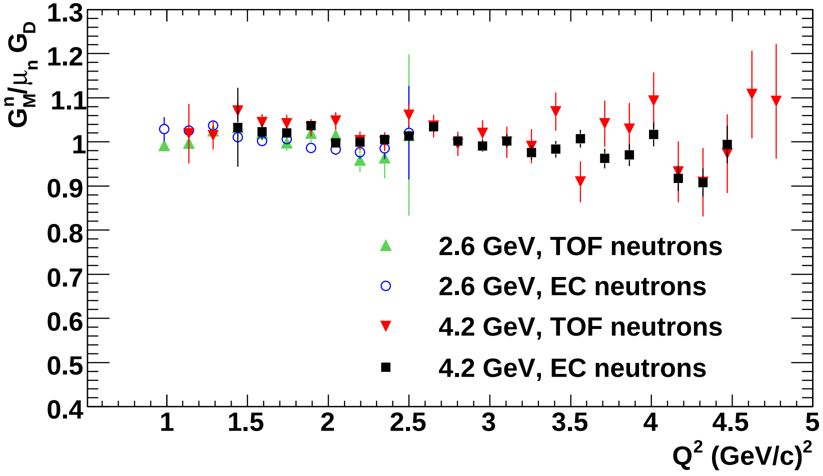

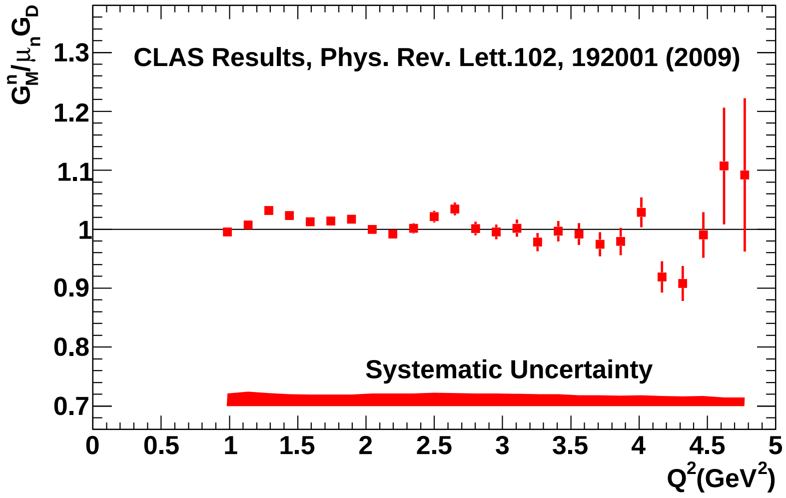

Comparison with Existing Data

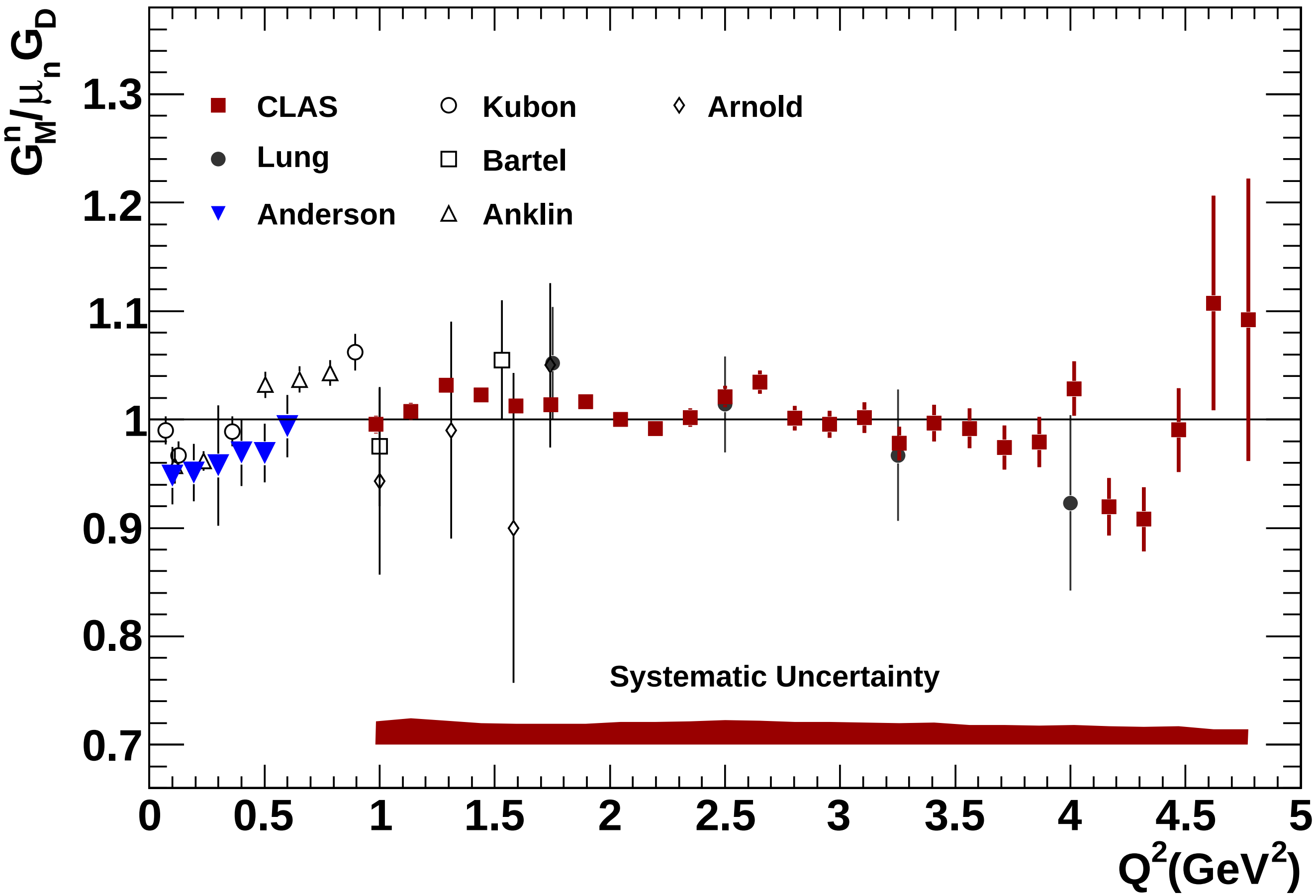

Comparison with Theory

- Green band - Diehl *et al.* (Eur. Phys. J. C 39, 1, 2005) use parameterized GPDs fitted to the data.
- Dashed curve - Guidal *et al.* (Phys. Rev. D 72, 054013, 2005) use a Regge parameterization of the GPDs to describe the elastic nucleon form factors at low Q^2 and extend it to higher Q^2.

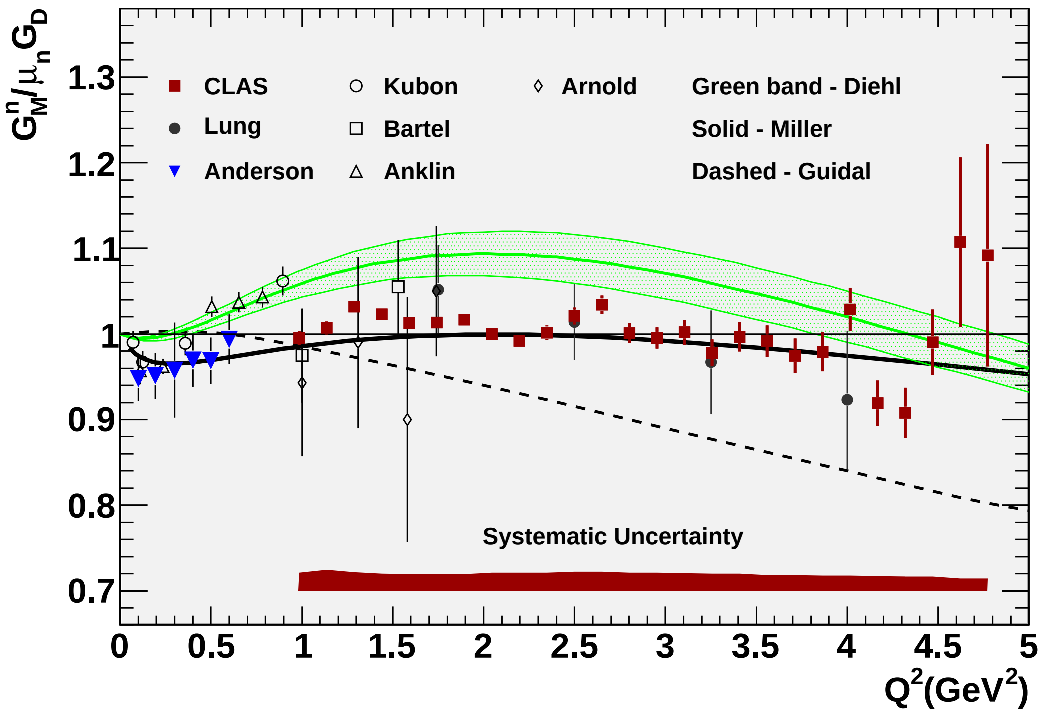

- Black curve - Miller's (Phys. Rev. C 66, 032201(R), 2002) uses light-front dynamics to describe a relativistic system of three bound quarks and a surrounding pion cloud.

Impact on World's Data for G_M^n

- Parameterization of world's data on G_M^n done by J.Kelly (PRC, 70, 068202, 2004) using the following function.

$$\frac{G_M^n}{\mu_n G_D} = \frac{\sum_{k=0}^{n} a_k \tau^k}{1 + \sum_{k=1}^{n+2} b_k \tau^k}$$

$$\tau = \frac{Q^2}{4M_p^2}$$

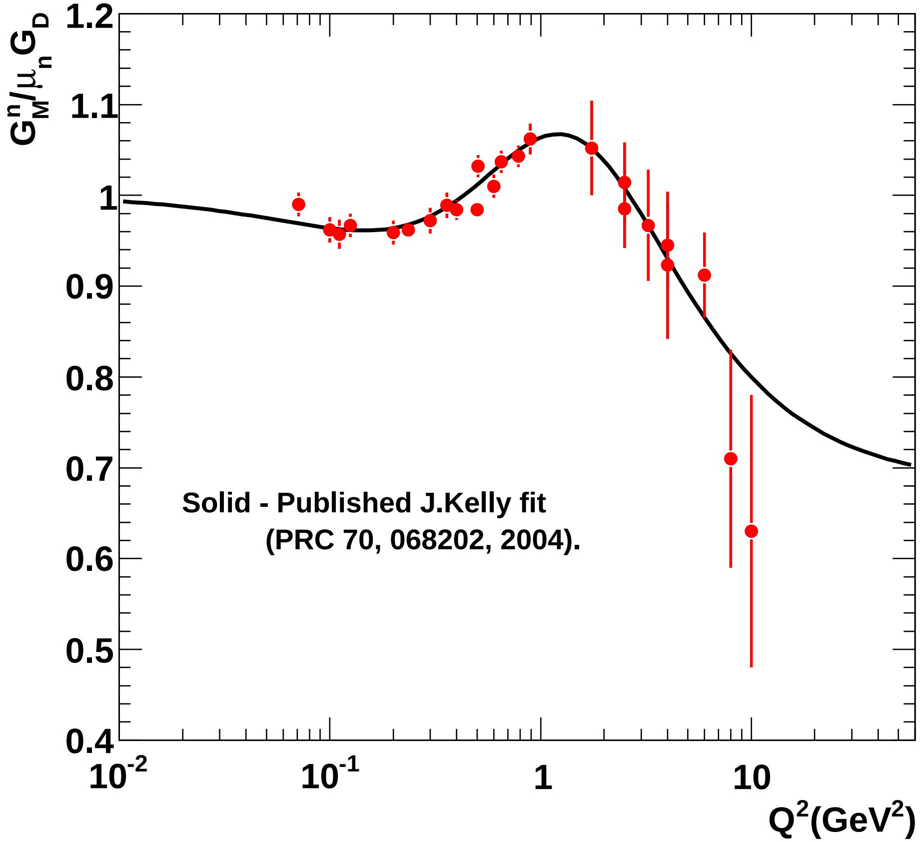

Impact on World's Data for G_M^n

- Parameterization of world's data on G_M^n done by J.Kelly (PRC, 70, 068202, 2004) using the following function.

$$\frac{G_M^n}{\mu_n G_D} = \frac{\sum_{k=0}^{n} a_k \tau^k}{1 + \sum_{k=1}^{n+2} b_k \tau^k}$$

$$\tau = \frac{Q^2}{4M_p^2}$$

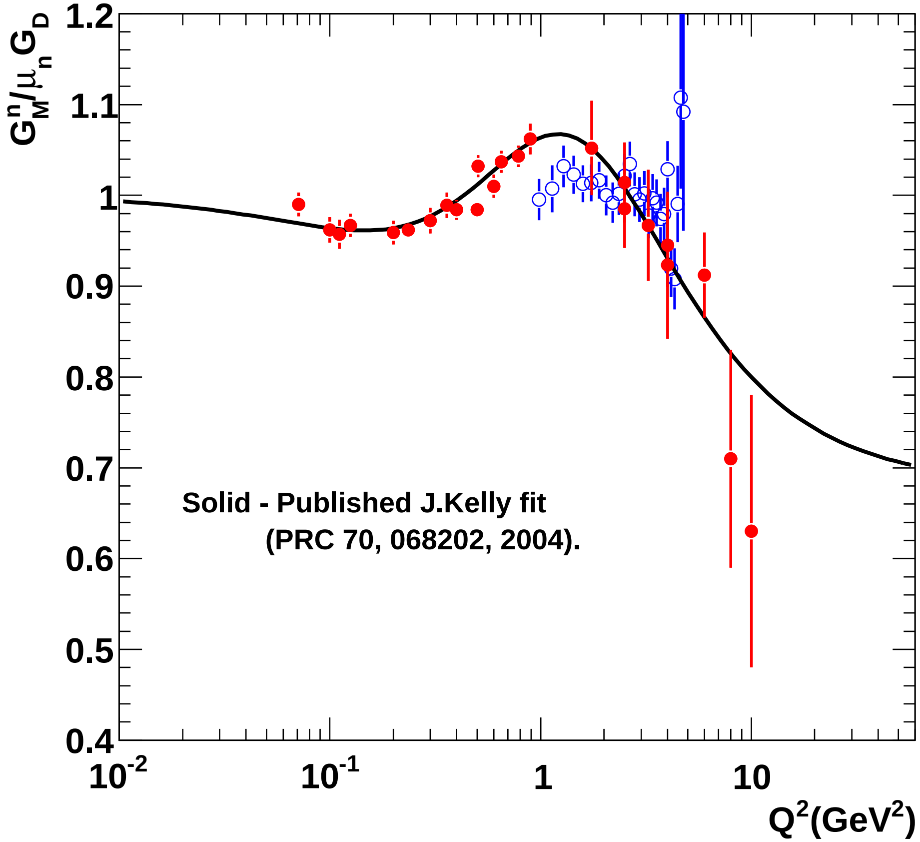

Impact on World's Data for G_M^n

- Parameterization of world's data on G_M^n done by J.Kelly (PRC, 70, 068202, 2004) using the following function.

$$\frac{G_M^n}{\mu_n G_D} = \frac{\sum_{k=0}^{n} a_k \tau^k}{1 + \sum_{k=1}^{n+2} b_k \tau^k}$$

$$\tau = \frac{Q^2}{4M_p^2}$$

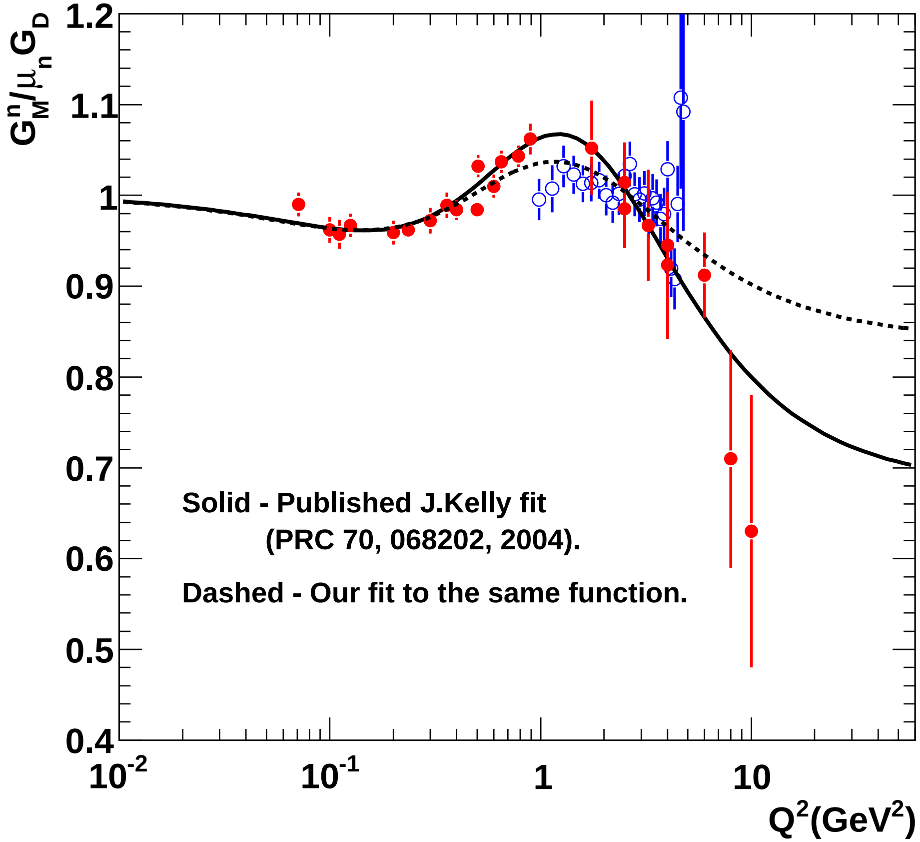

Effect of CLAS Data on Miller* Calculation

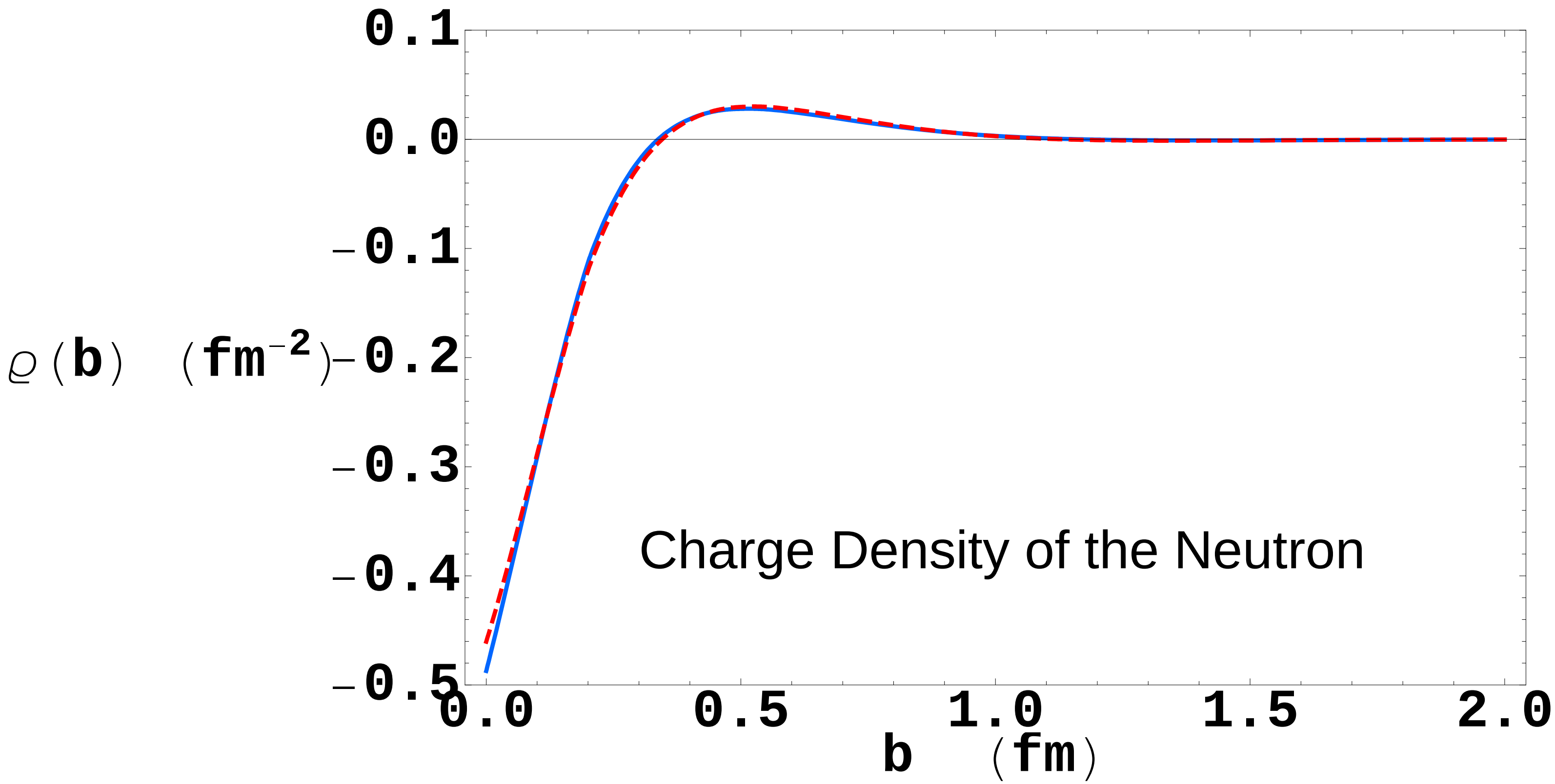

* G.Miller, private communication.

Status and Future Plans

- Published in Phys. Rev. Lett.102, 192001 (2009).
- The reversed-torus-polarity data are still being analyzed.
- A proposal to measure G_M^n at 12 GeV was approved by the JLab PAC in August, 2007. The expected data range and uncertainties are shown below.

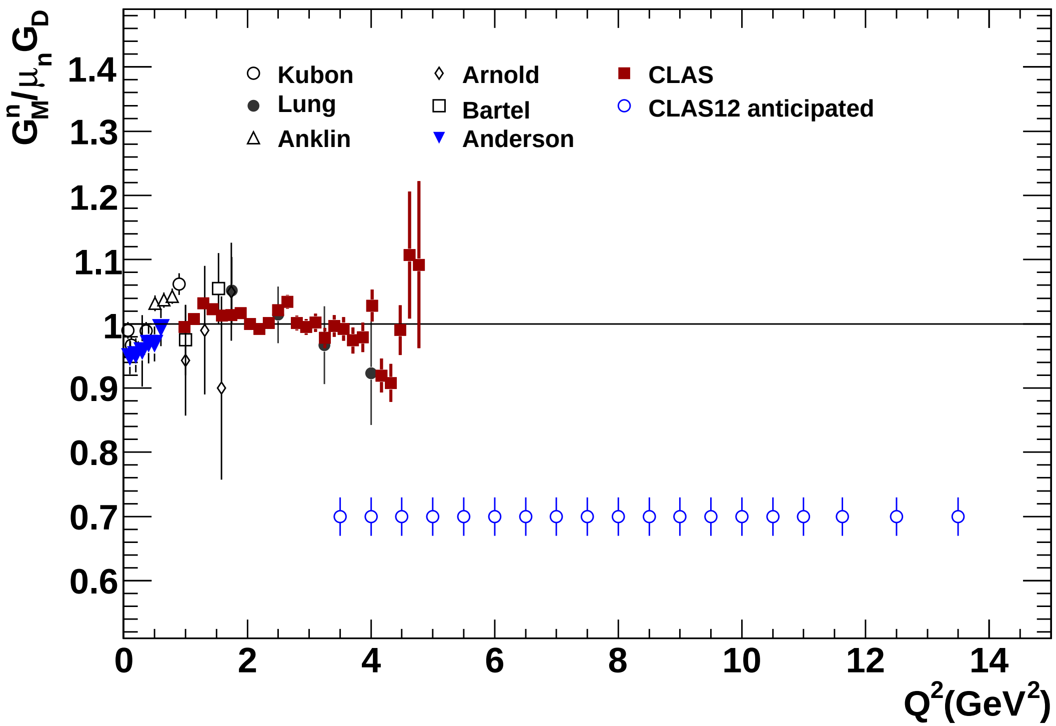

Conclusions

- We have measured the neutron magnetic form factor G_M^n over the range $\mathrm{Q}^2 = 1.0 - 4.8\ (\mathrm{GeV/c})^2$ to a precision better than 2.5%.
- The four different measurements of G_M^n at two beam energies with the calorimeter and the TOF system in CLAS are consistent with each other and with previous results in this Q^2 range.
- The results are consistent with the dipole approximation within 5% across almost the full range of Q^2; differing from many expectations.
- Light-cone calculation by Miller gives the best description of the full G_M^n dataset.
- Kelly parameterization of G_M^n changes significantly with the new CLAS data, but this difference has surprisingly little effect on the neutron charge distribution extracted by Jerry Miller.

Some History

PHYSICAL REVIEW C VOLUME 46, NUMBER 1 JULY 1992

Heavy residue production in 215 MeV $^{16}O + ^{27}Al$ reactions

G. P. Gilfoyle,* M. S. Gordon,† and R. L. McGrath
Department of Physics, State University of New York at Stony Brook, Stony Brook, New York 11794

G. Auger‡ and J. M. Alexander
Department of Chemistry, State University of New York at Stony Brook, Stony Brook, New York 11794

D. G. Kovar,§ M. F. Vineyard,† C. Beck,** and D. J. Henderson
Argonne National Laboratory, Argonne, Illinois 60439

P. A. DeYoung and D. Kortering
Department of Physics, Hope College, Holland, Michigan 49423
(Received 15 January 1992)

Mass, velocity, and angular distributions have been measured for heavy products and for light charged particles from the reaction 215 MeV $^{16}O + ^{27}Al$. Coincidences between evaporation residues and light charged particles have also been measured. Statistical-model calculations, incorporating light-particle decay from either the compound nucleus or the composite nucleus formed in the direct emission of a beam velocity particle, cannot account for the observed cross sections or angular distributions of the heavy residues. More elaborate kinematic simulations, which include direct light-particle emission as observed in the light-particle inclusive data, also do not work. This supports the notion that heavy fragment production ($A > 4$) would be needed to account for the residue distributions.

Some History

PHYSICAL REVIEW C VOLUME 46, NUMBER 1 JULY 1992

Heavy residue production in 215 MeV $^{16}O + ^{27}Al$ reactions

G. P. Gilfoyle,* M. S. Gordon,† and R. L. McGrath
Department of Physics, State University of New York at Stony Brook, Stony Brook, New York 11794

G. Auger‡ and J. M. Alexander
Department of Chemistry, State University of New York at Stony Brook, Stony Brook, New York 11794

D. G. Kovar,§ M. F. Vineyard,† C. Beck,** and D
Argonne National Laboratory, Argonne, Illinois

P. A. DeYoung and D. Kortering
Department of Physics, Hope College, Holland, Mic
(Received 15 January 1992)

Mass, velocity, and angular distributions have been measured for heav
particles from the reaction 215 MeV $^{16}O + ^{27}Al$. Coincidences betwee
charged particles have also been measured. Statistical-model calculati
decay from either the compound nucleus or the composite nucleus fo
beam velocity particle, cannot account for the observed cross section
heavy residues. More elaborate kinematic simulations, which include
observed in the light-particle inclusive data, also do not work. This sup
ment production ($A > 4$) would be needed to account for the residue dis

MOMENTUM SPECTRUM OF

$np(n_S) \rightarrow nn\pi^+(n_S)^*$

by

Gerard P. Gilfoyle**
Franklin & Marshall College
Lancaster, PA

under the supervision of

A. Snyder

Bubble Chamber Group
High Energy Physics Division
Argonne National Laboratory

Some History

PHYSICAL REVIEW C VOLUME 46, NUMBER 1 JULY 1992

Heavy residue production in 215 MeV $^{16}O + ^{27}Al$ reactions

G. P. Gilfoyle,* M. S. Gordon,† and R. L. McGrath
Department of Physics, State University of New York at Stony Brook, Stony Brook, New York 11794

G. Auger‡ and J. M. Alexander
Department of Chemistry, State University of New York at Stony Brook, Stony Brook, New York 11794

D. G. Kovar,§ M. F. Vineyard,† C. Beck,** and D
Argonne National Laboratory, Argonne, Illinoi

P. A. DeYoung and D. Kortering
Department of Physics, Hope College, Holland, Mic

(Received 15 January 1992)

Mass, velocity, and angular distributions have been measured for hea
particles from the reaction 215 MeV $^{16}O + ^{27}Al$. Coincidences betwee
charged particles have also been measured. Statistical-model calculat
decay from either the compound nucleus or the composite nucleus fo
beam velocity particle, cannot account for the observed cross section
heavy residues. More elaborate kinematic simulations, which include
observed in the light-particle inclusive data, also do not work. This sup
ment production ($A > 4$) would be needed to account for the residue dis

MOMENTUM SPECTRUM OF

$np(n_S) \rightarrow nn\pi^{+}(n_S)$*

by

Gerard P. Gilfoyle**
Franklin & Marshall College
Lancaster, PA

under the supervision of

on
y

*Work performed at Argonne National Laboratory, a contract laboratory of the United States Department of Energy
**Participant in the Spring 1978 Undergraduate Research Participation Program, January 9-April 28, 1978. This program is coordinated by the Argonne Center for Educational Affairs.

Additional Slides

Radiative Corrections

- Radiative corrections: Calculated for exclusive $D(e,e'p)n$ with the code EXCLURAD (CLAS-Note 2005-022 and A.Afanasev, I.Akushevich, V.Burkert, and K.Joo, Phys.Rev., D66, 074004, 2002).
- Ratio of $e-n/e-p$ corrections close to unity.

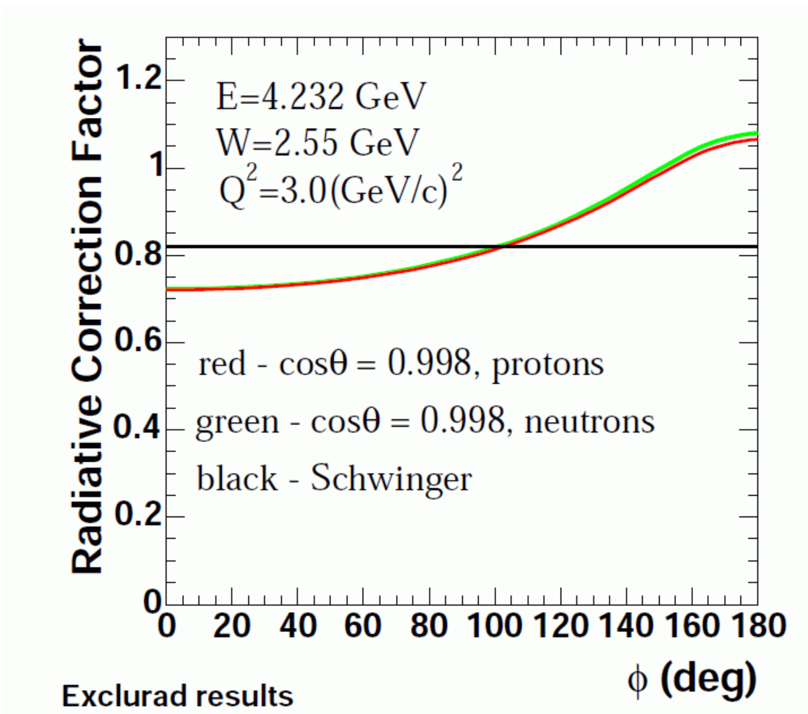

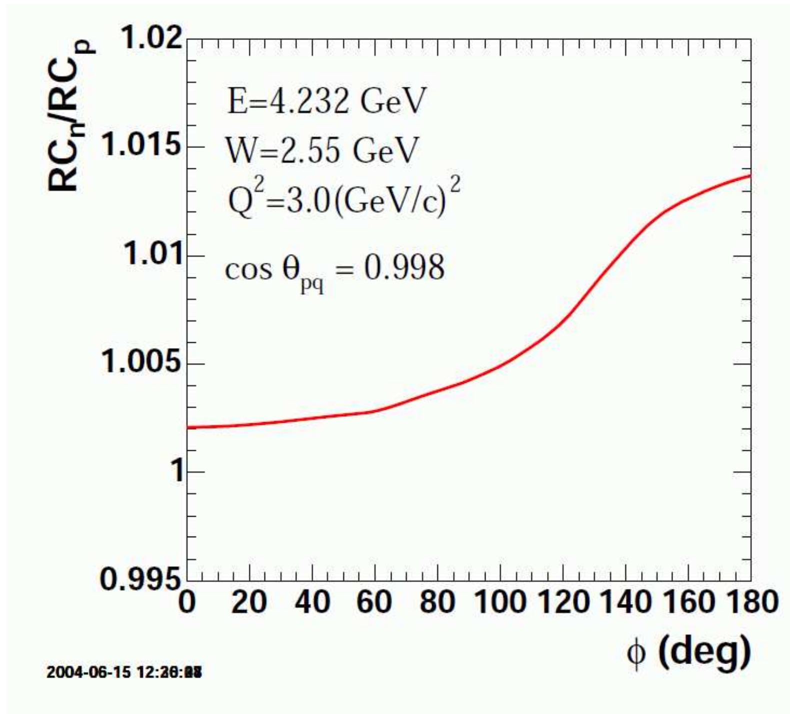

Nuclear Corrections

- The cross section was calculated using the Plane Wave Impulse Approximation (PWIA) for $Q^2 \geq 1.0\ \mathrm{GeV}^2$, the AV18 deuteron wave function (R. Wiringa et al., Phys. Rev. C 51, 38, 1995), and Glauber theory for final-state interactions (FSI).
- The correction is the ratio of the full calculation to the PWIA without FSI.
- The correction was averaged over the same θ_{pq} range used in the analysis and was less than 0.1% across the full Q^2 range.

Nuclear corrections to R from the Jeschonnek model.

Q^2	$f_{nuclear}$
1	0.999796
2	0.999714
3	0.999655
4	0.999624
5	0.999619

Lomon Calculations

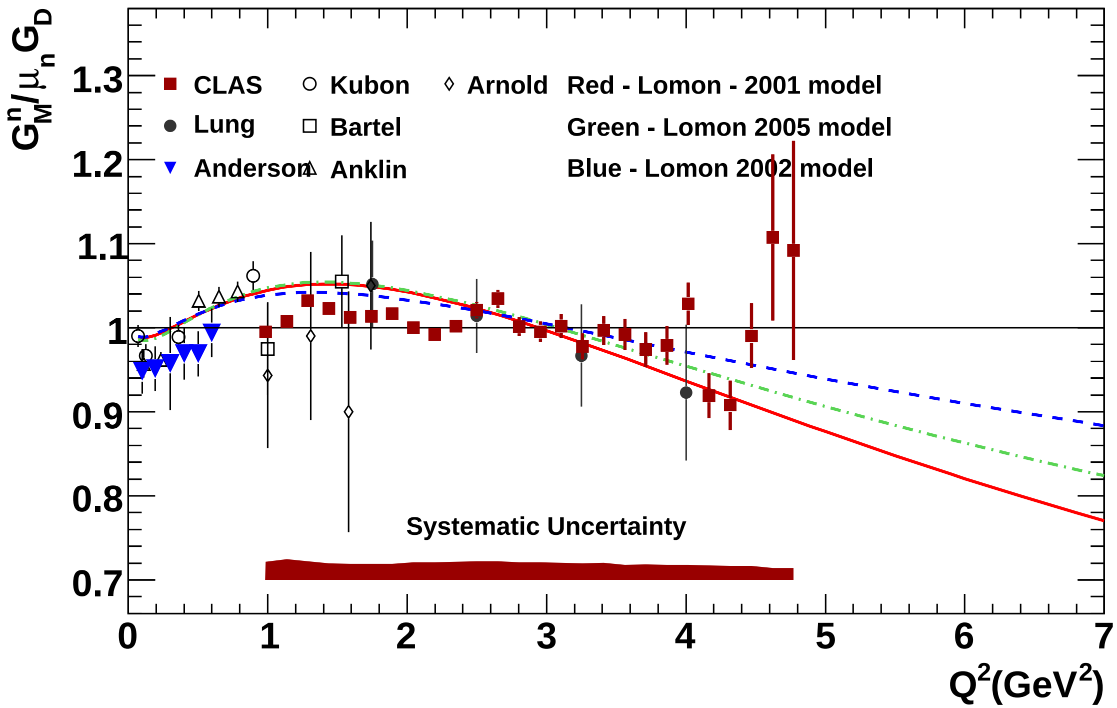

- 2001 Model - Used dcs(?) (Rosenbluth) data for G_E^n and G_E^p and no polarization data.
- 2005 Model - Gives same result for G_M^n as 2008 model which included low Q^2 $R_n = \mu_n G_E^p / G_M^n$ and $R_p = \mu_p G_E^n / G_M^n$ results from BLAST and preliminary, high-Q^2 results for R_n from JLab.
- 2002 Model

Miller Calculations

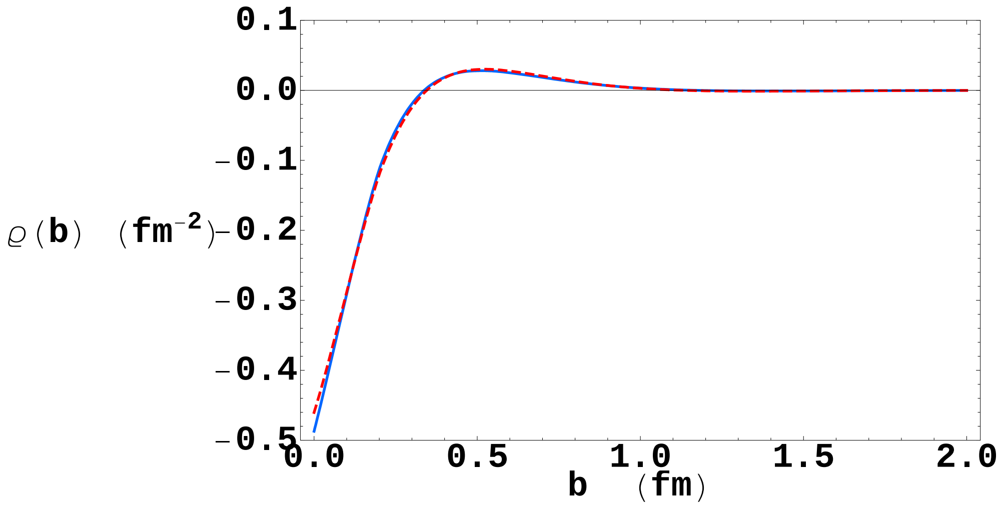

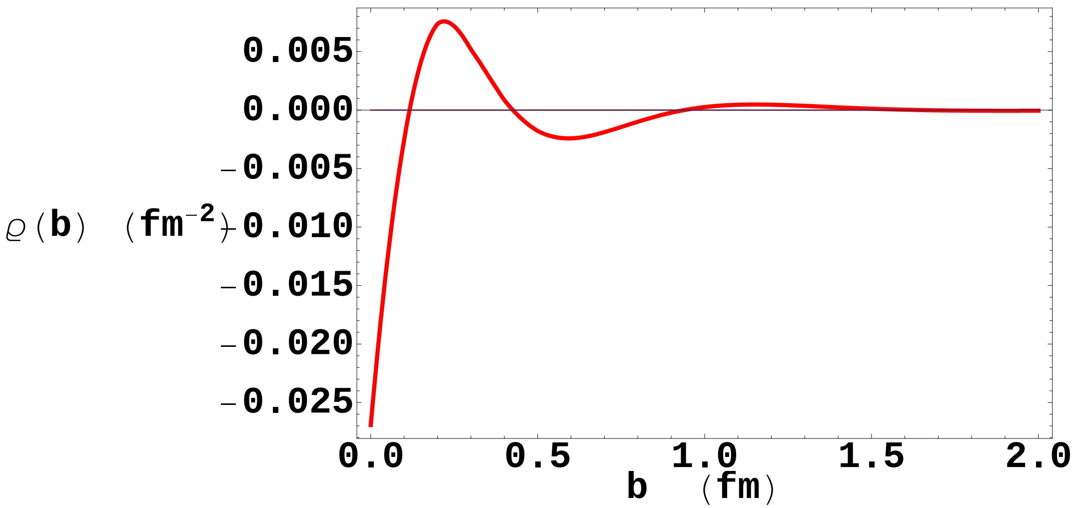

Fermi Correction

Fermi motion in the target: Causes nucleons to migrate out of the CLAS acceptance. Effect was simulated.

TOF (2.6 GeV)

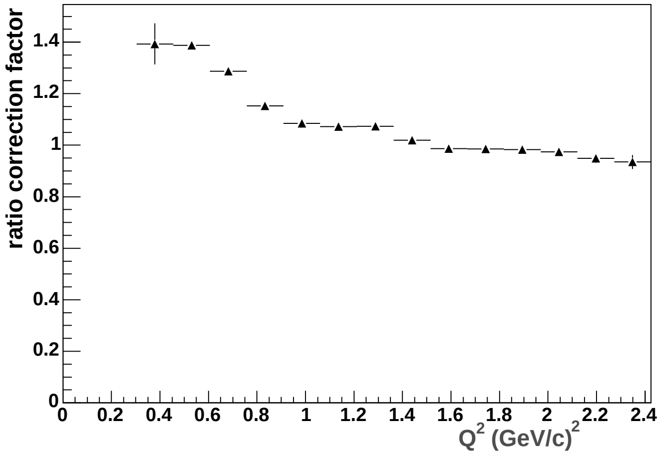

Calorimeter (2.6 GeV)

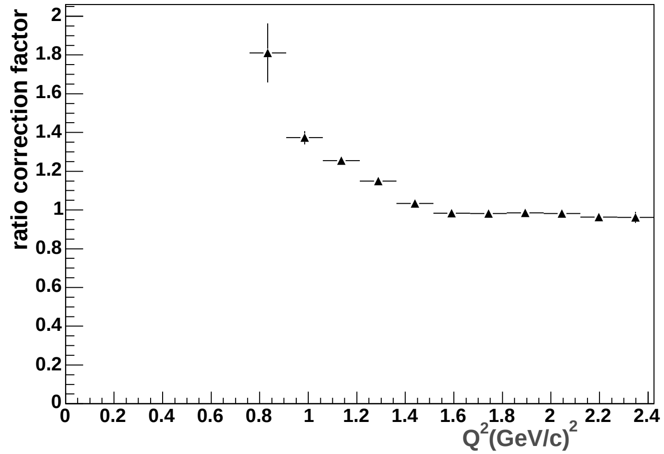

Effect of Fermi Correction

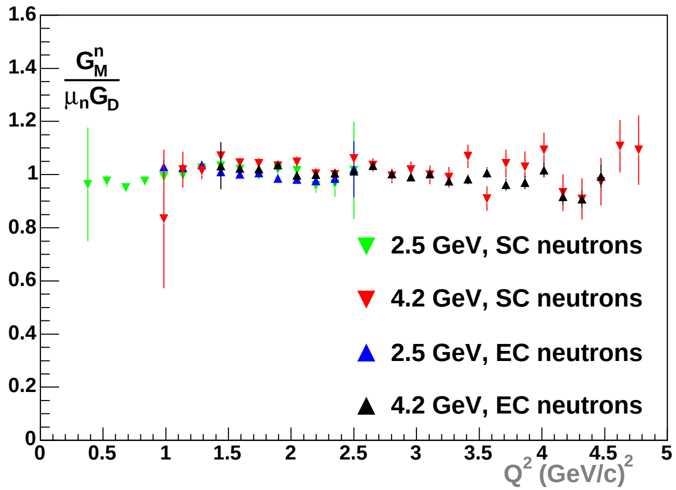

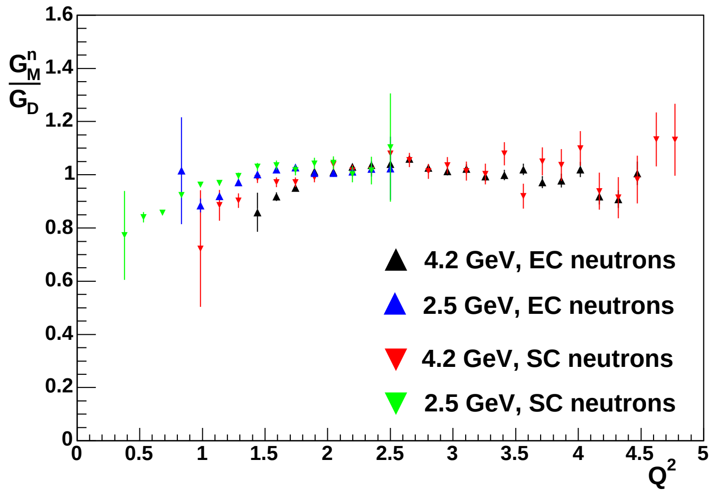

Reduced G_M^n for four different measurements.

Reduced G_M^n for four different measurements. The Fermi corrections have not been applied.

Monte Carlo Simulation

- Study quasielastic and inelastic scattering from both neutron and proton. The inelastic scattering produces a background that overlaps with the quasielastic events.
- For quasielastic scattering use the elastic nucleon form factors to get the cross section on the nucleon and then incorporate the effects of the target nucleon’s Fermi motion inside the deuteron.
- For inelastic scattering use existing proton and deuteron data to parameterize the cross sections for both protons and neutrons and add the Fermi motion.

Procedure for Quasielastic Simulation

- Pick a Q^2 weighted by the elastic cross section.
- Pick p_f and $\cos\theta$ of the target nucleon weighting it by the combination of the Hulthen distribution and the effective-beam-energy effect.
- Boost to the rest frame of the nucleon and rotate coordinates so the beam direction is along the z axis. Calculate a new beam energy in the nucleon rest frame.
- Choose an elastic scattering angle in the nucleon rest frame using the Brash parameterization.
- Transform back to the laboratory frame.

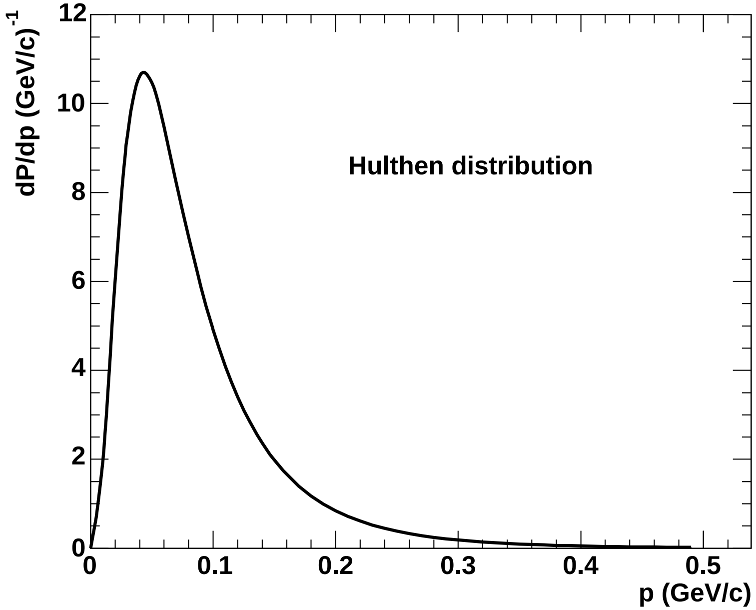

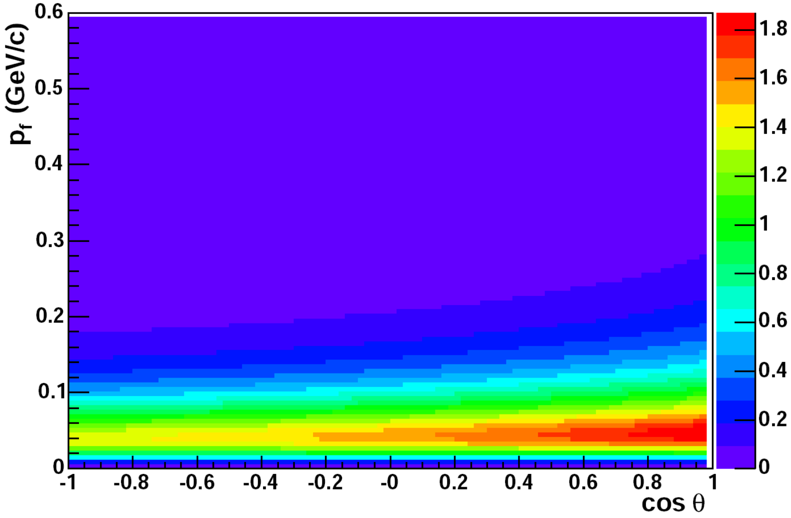

Procedure for Inelastic Simulation - 1

- Use existing measurements of inelastic scattering on the proton (P. Stoler, Phys. Rep., **226**, 103 (1993)).
- For the neutrons use inelastic scattering from deuterium (L.M.Stuart, *et al.*, Phys. Rev. **D58** (1998) 032003). Data don't cover the full CLAS12 range, but $n-p$ ratios are roughly constant.

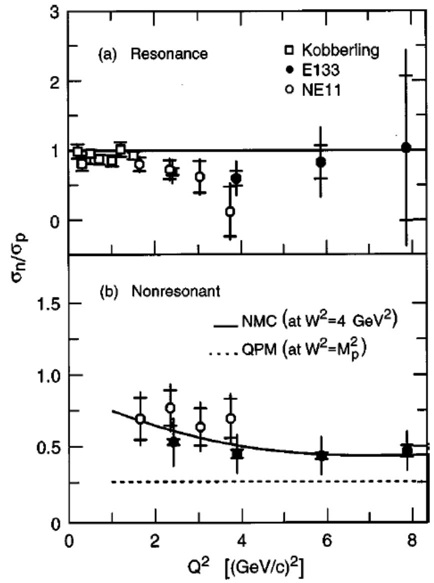

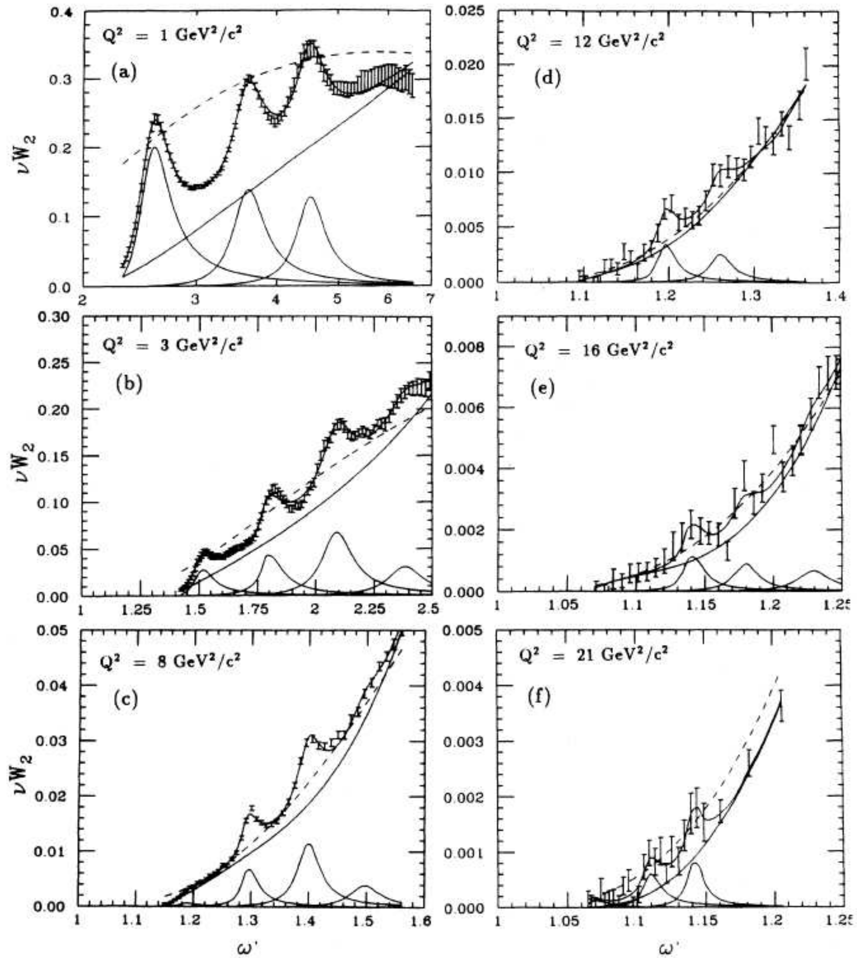

Inelastic cross sections as a function of $\omega' = 1 + W^2/Q^2$.

Procedure for Inelastic Simulation - 2

- Pick a Q^2 weighted by the measured cross sections.
- Pick p_f and $\cos\theta$ of the nucleon weighted by the Hulthen distribution and the effective-beam-energy effect for inelastic scattering.
- Boost to the rest frame of the nucleon and rotate coordinates so the beam direction is along the z axis. Calculate a new beam energy in the nucleon rest frame.
- Choose the final state using genev (M.Ripani and E.N.Golovach based on P.Corvisiero, et al., NIM A**346**, (1994) 433.).
- Transform back to the laboratory frame.

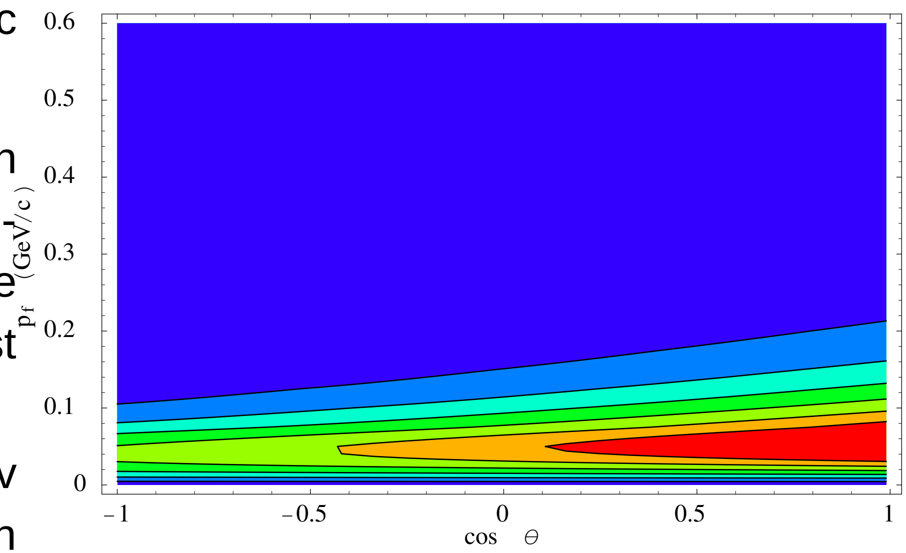

NDE Coverage from $^{1}\mathrm{H}(e, e'\pi^{+})\mathrm{n}$

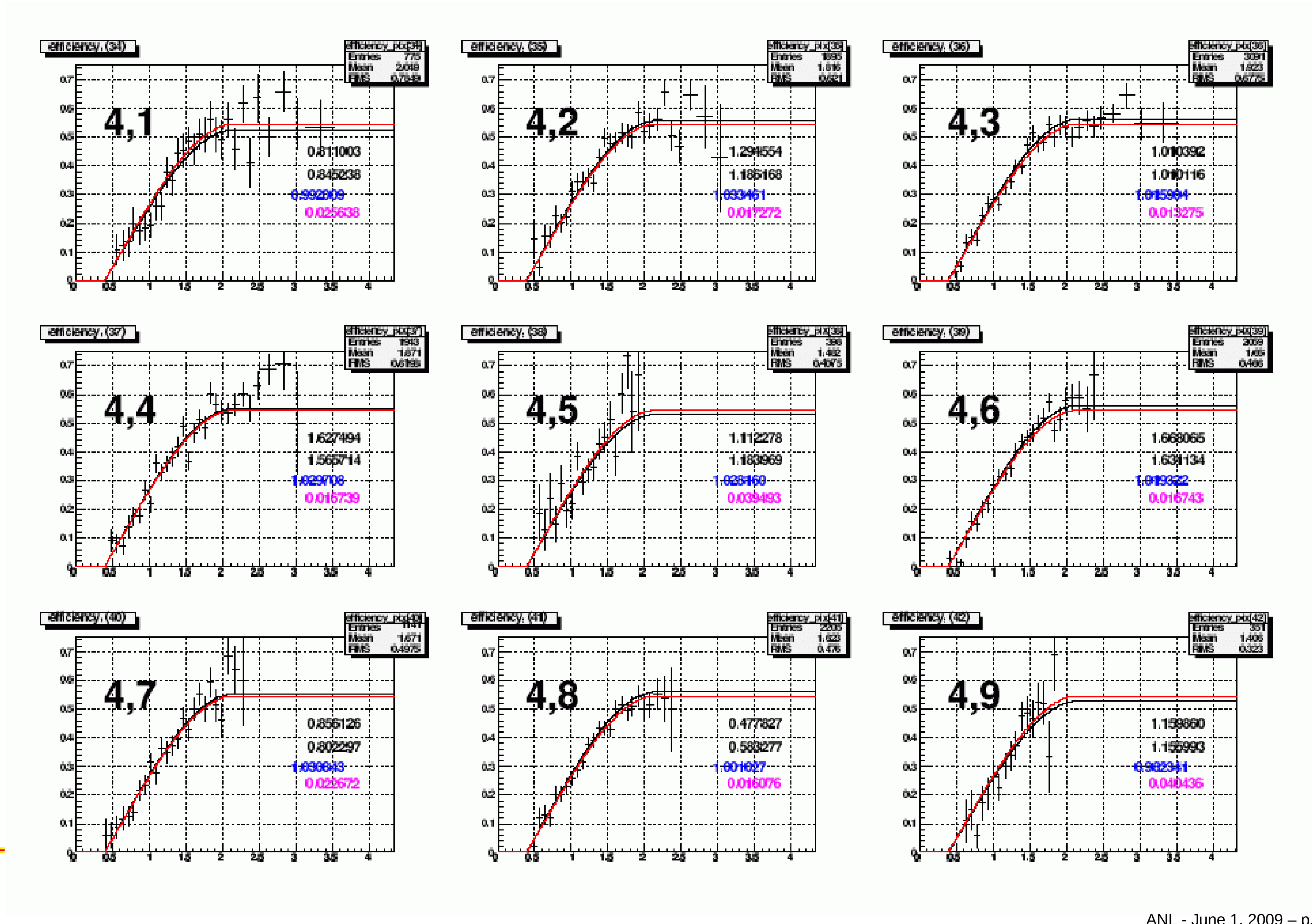

Published Measurements of Elastic Form Factors

- G_M^n
- G_M^p
- G_E^p/G_M^p

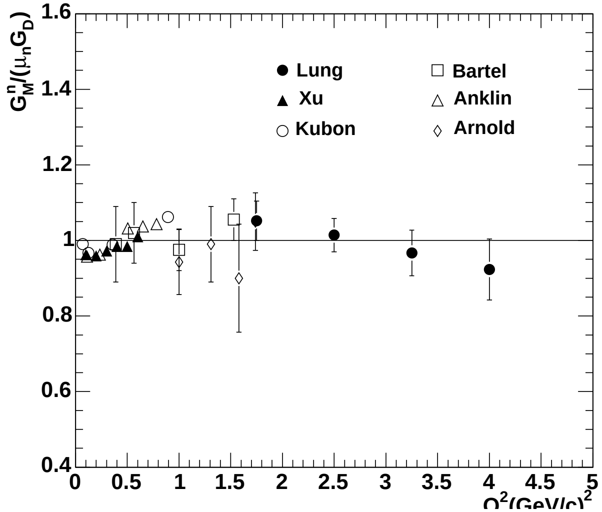

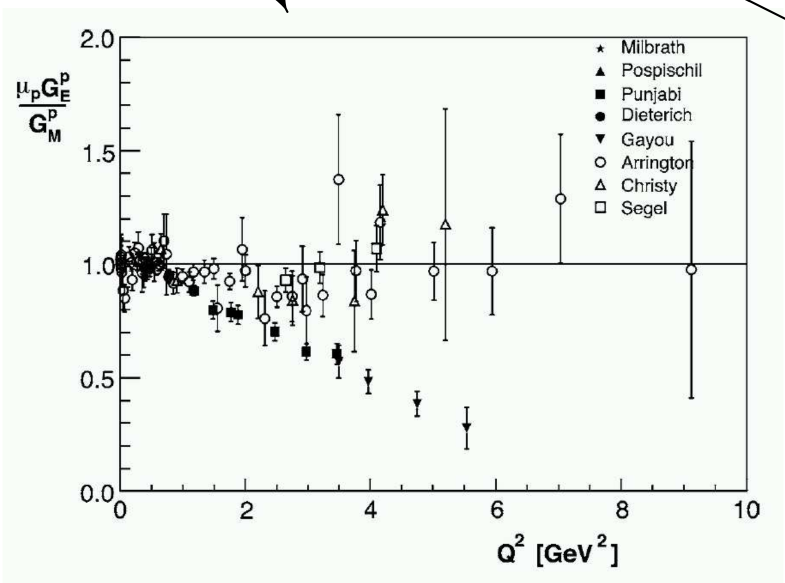

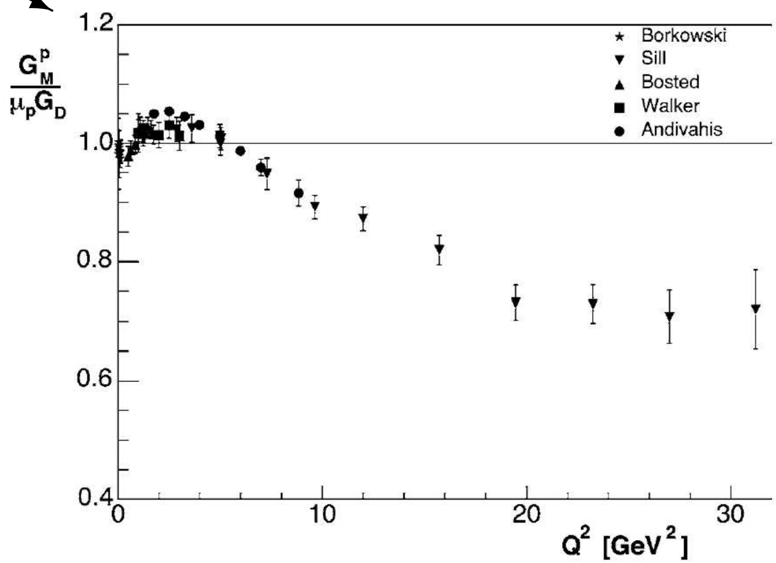

C.E. Hyde-Wright and K.deJager, Ann. Rev. Nucl. Part. Sci. **54** (2004) 54.

Systematic Errors

- Calorimeter neutron detection efficiency parameterization: The neutron efficiency was fitted with a third order polynomial plus a flat region at higher momentum. To study systematic uncertainties the highest order term was dropped and the ratio R regenerated. The upper limit on the range of differences for the different extractions of R was assigned the systematic uncertainty.
- TOF neutron detection efficiency parameterization: Similar to calorimeter extraction except the second and third order terms in the polynomial were dropped.

Detector	2.6 GeV	4.2 GeV
Calorimeter	1.5	1.0
TOF	2.0	3.2

Percentage systematic uncertainties in neutron efficiency parameterization.

- These are the largest contributions from this measurement.

Reducing SC Background

1. Cut on the time difference between the measured TOF and the predicted TOF using the neutron momentum extracted from the missing momentum.
2. Require a minimum of 5 MeV (electron equivalent) in the SC to reject low-energy photons.

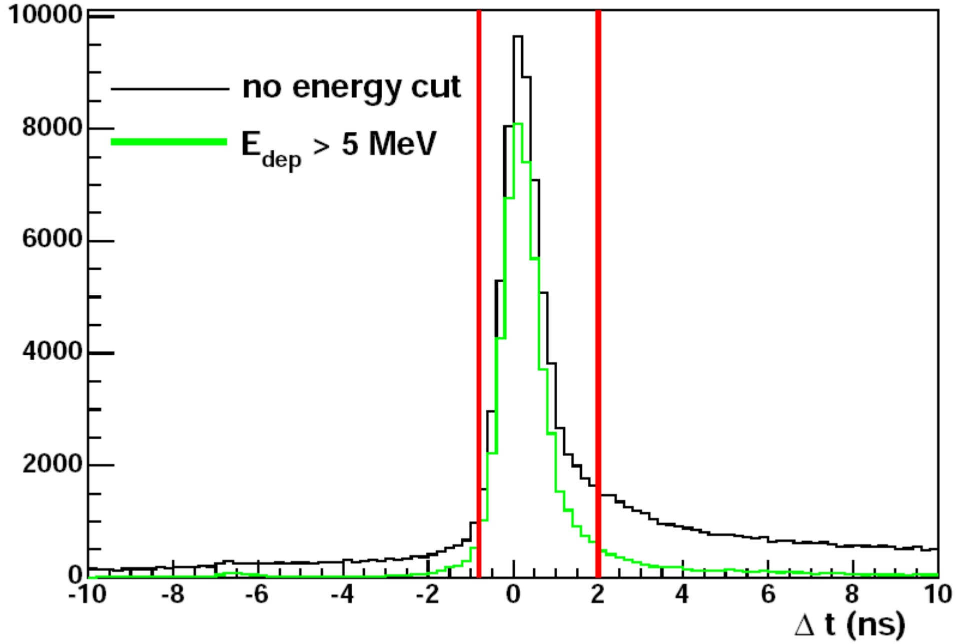

Results - Systematic Uncertainties

- Individual contributions to the systematic uncertainty for all four measurements (2.6 GeV EC and TOF and 4.2 GeV EC and TOF) were added in quadrature.
- Final, combined systematic uncertainty was the weighted average of all four measurements: $\delta G_M^n / G_M^n \times 100 < 2.5\%$.

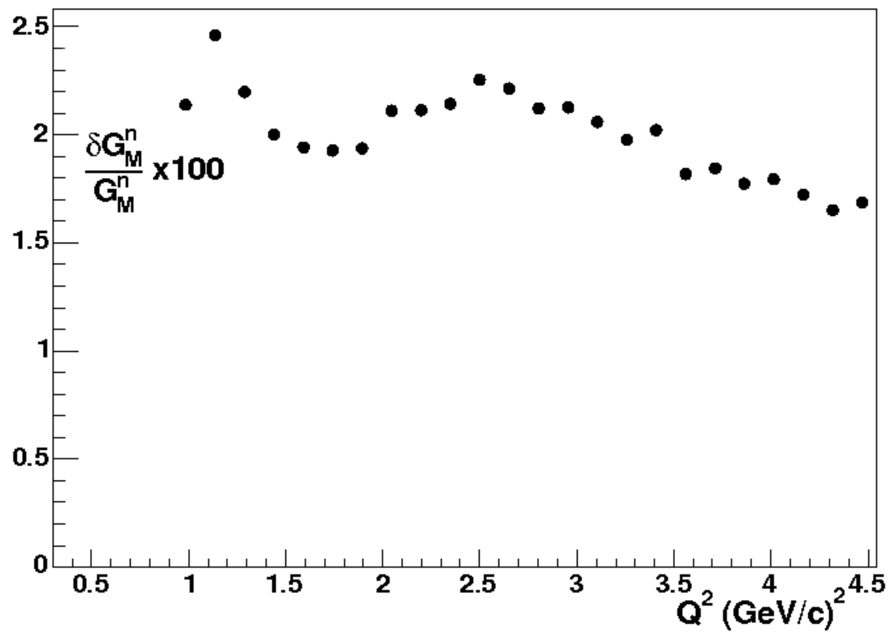

The Ratio Method - Extracting G_M^n

- Rearrange the expression for R to determine G_M^n.

$$G_M^n = \sqrt{R\frac{\frac{1}{\sigma_{Mott}}\frac{1}{a(E,Q^2,\theta_{pq}^{max},W_{max}^2)}\frac{d\sigma}{d\Omega}[^1\mathrm{H}(e,e')p] - \frac{1}{1+\tau}\left(G_E^n\right)^2}{\frac{\tau}{1+\tau}+2\tau\tan^2\frac{\theta}{2}}}$$

- The ratio R depends on a set of parameters f_i so the uncertainty on G_M^n is the following.

$$\left(\delta G_M^n\right)^2 = \sum_i \left(\frac{\partial G_M^n}{\partial f_i}\right)^2 \left(\delta f_i\right)^2$$

Anklin *et al.* and Kubon *et al.* Measurements

- Used the ratio method to measure G_M^n.
- Neutrons detected in scintillator array consisting of thick E and thin ΔE counters.
- Protons detected in same scintillator array using the energy TOF and the E signals.
- Neutron detection efficiency measurement performed at the Paul Scherrer Institute.
  - High (low) energy neutron beam produced in the $^{12}\mathrm{C(p,n)}$ ($\mathrm{D(p,n)}$) reaction and then scattered off a liquid $\mathrm{H_2}$ target.
  - Neutrons scattering off the liquid $\mathrm{H_2}$ target were tagged by detecting the recoil proton from the $\mathrm{H(n,p)n}$ reaction.
  - Final sample of tagged neutrons used to measure NDE.

Systematic Uncertainties - NDE

- Calorimeter neutron detection efficiency (NDE) parameterization: NDE fitted with a third order polynomial plus a flat region at higher momentum. Highest order term was dropped and the ratio R regenerated. Fits for 4.2-GeV EC data shown in top panel.
- TOF NDE parameterization: Similar to calorimeter extraction except the second and third order terms in the polynomial were dropped. Fits for 4.2-GeV SC data in bottom panel with production fit (left) and modified fit (right).

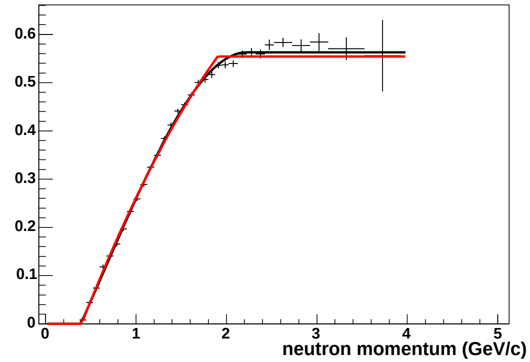

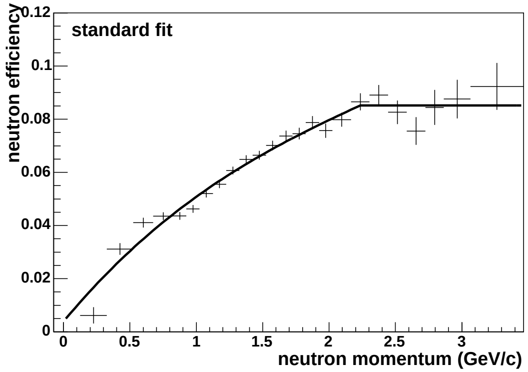

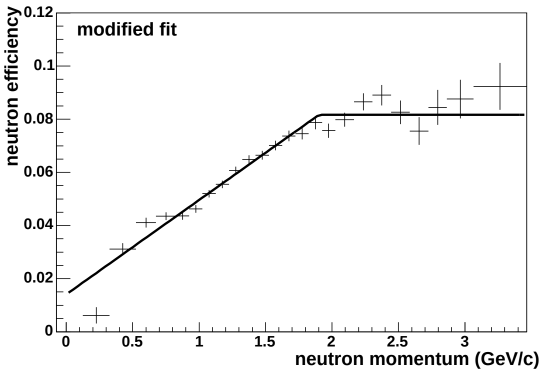

EEFFs and lattice QCD